Received: 6 January 2020 | Revised: 8 May 2020 | Accepted: 9 May 2020

DOI: 10.1096/fj.202000030RR

RESEARCH ARTICLE

THE FASEB JOURNAL

Polyunsaturated fatty acid deficiency affects sulfatides and other sulfated glycans in lysosomes through autophagy-mediated degradation

Yaping Wang[1] | Takero Nakajima[1] | Pan Diao[1] | Yosuke Yamada[1,2] | Kozo Nakamura[3] | Jun Nakayama[4] | Naoki Tanaka[1] | Toshifumi Aoyama[1] | Yuji Kamijo[1,2]

[1]Department of Metabolic Regulation, Shinshu University School of Medicine, Matsumoto, Japan

[2]Department of Nephrology, Shinshu University School of Medicine, Matsumoto, Japan

[3]Department of Bioscience and Biotechnology, Faculty of Agriculture, Shinshu University, Minamiminowa, Japan

[4]Department of Molecular Pathology, Shinshu University School of Medicine, Matsumoto, Japan

Correspondence
Yuji Kamijo, Department of Nephrology, Shinshu University School of Medicine, 3-1-1 Asahi, Matsumoto, Nagano 390-8621, Japan.
Email: yujibeat@shinshu-u.ac.jp

Funding information
Grant-in-Aid for Scientific Research (Kakenhi) in Japan, Grant/Award Number: 18K08204

Abstract

Metabolic changes in sulfatides and other sulfated glycans have been related to various diseases, including Alzheimer's disease (AD). However, the importance of polyunsaturated fatty acids (PUFA) in sulfated lysosomal substrate metabolism and its related disorders is currently unknown. We investigated the effects of deficiency or supplementation of PUFA on the metabolism of sulfatides and sulfated glycosaminoglycans (sGAGs) in sulfatide-rich organs (brain and kidney) of mice. A PUFA-deficient diet for over 5 weeks significantly reduced the sulfatide expression by increasing the sulfatide degradative enzymes arylsulfatase A and galactosylceramidase in brain and kidney. This sulfatide degradation was clearly associated with the activation of autophagy and lysosomal hyperfunction, the former of which was induced by suppression of the Erk/mTOR pathway. A PUFA-deficient diet also activated the degradation of sGAGs in the brain and kidney and that of amyloid precursor proteins in the brain, indicating an involvement in general lysosomal function and the early developmental process of AD. PUFA supplementation prevented all of the above abnormalities. Taken together, a PUFA deficiency might lead to sulfatide and sGAG degradation associated with autophagy activation and general lysosomal hyperfunction and play a role in many types of disease development, suggesting a possible benefit of prophylactic PUFA supplementation.

KEYWORDS

amyloid precursor protein, Erk1/2, glycosaminoglycans, lysosome enzyme, mTOR, nutritional deprivation

Abbreviations: AD, Alzheimer's disease; AMPKα, AMP-activated protein kinase α; APP, amyloid precursor protein; Aβ, amyloid β; ARSA, arylsulfatase A; CGT, ceramide galactosyltransferase; CST, cerebroside sulfotransferase; CS, chondroitin sulfate; CLEAR, coordinated lysosomal expression and regulation; DS, dermatan sulfate; Erk1/2, extracellular regulated protein kinase-1/2; FA, fatty acids; GALC, galactosylceramidase; GAG, glycosaminoglycan; HS, heparan sulfate; HCO, hydrogenated coconut oil; KS, keratan sulfate; LAMP-1, lysosome associated membrane protein type 1; LC3B, microtubule associated protein 1 light chain 3B; LS, lysosulfatides; mTOR, mammalian target of rapamycin; PBS, phosphate buffer solution; PD, Parkinson's disease; PUFA, polyunsaturated fatty acids; TFEB, transcription factor EB; TBS, Tris-buffered saline; UPS, ubiquitin-proteasome system.

1 | INTRODUCTION

Sulfatides, or 3-O-sulfogalactosylceramides, are sulfated glycosphingolipids composed of fatty acids (FA), galactose, sphingosine, and sulfate. Sulfatides are found at the extracellular leaflet of the plasma membrane in most eukaryotic cells and are highly expressed in the mammalian brain and kidney.[1] Sulfatides were first isolated from human brain tissue by Thudichum in 1884.[2,3] Since then, the potential roles of sulfatides in the nervous system, immune system, glucose metabolism, osmotic regulation, spermatogenesis, thrombosis/hemostasis, and bacterial and viral infections have been reported by numerous studies.[4-6] In the nervous system, sulfatides are abundant in myelin and comprise 4% of total myelin lipids.[3] Earlier investigations described that decreased in sulfatides in the cerebrospinal fluid could be a useful biomarker for white matter lesions.[7] In Alzheimer's disease (AD), a marked decrease in brain sulfatide level has been proved to be associated with early phase of pathological process of AD. The depletion of sulfatides and elevation of ceramide, a premetabolite of sulfatides, occurred mainly in the cerebral gray matter prior to other lipid abnormalities, and these lipid changes contributed to neurodegeneration in AD.[8,9] In Parkinson's disease (PD), it was also found that sulfatides were considerably diminished in the frontal cortex.[10] In the kidney, sulfatides also play important physiological roles in acid-base homeostasis via urinary acidification and ammonium handling as well as in the transport of sodium chloride.[11,12] Several studies have proposed that disturbances in sulfatide metabolism might be associated with such kidney diseases as renal cell carcinoma and polycystic kidney disease.[13,14]

Sulfated glycans, currently explored in medicine as glycosaminoglycans (GAGs), are also known to contribute to numerous pathophysiological processes. In the nervous system, GAGs reportedly play many critical roles, including regulation of the proliferation and differentiation of neural progenitor cells, neuronal migration, neural regeneration and plasticity, synaptogenesis, and axon pathfinding.[15,16] Therefore, disturbances in GAG homeostasis are associated with many brain diseases. GAGs also play a vital part in kidney function homeostasis. GAGs are distributed over nephrons and can bind and regulate a variety of proteins, such as cytokines, growth factors, and enzymes, and their abnormal expression influences fibrosis and inflammation.[17] Alterations in GAG structure and/or content have been investigated in a large number of kidney pathologies, including polycystic kidney disease, diabetic nephropathy, nephroblastoma (Wilms' tumor), amyloidosis, minimal-change nephropathy, Denys-Drash syndrome, and glomerulonephritides.[18] GAGs are suggested to contribute to the normal function of filtration barriers in kidney glomeruli and protection from tubular injury and interstitial fibrosis.[19]

These sulfated substrates, sulfatides, and other sulfated glycans are degraded in lysosomes. A breakdown in their metabolic homeostasis is thought to influence the development of many diseases. However, the key factors affecting the intracellular metabolism of sulfated lysosomal substrates are not fully understood.

Lipid homeostasis is essential for good health, with lipid metabolism dysregulation involved in the development of many human diseases. Essential polyunsaturated fatty acids (PUFA) from n-6 and n-3 FA are linoleic (18:2, n-6) and linolenic (18:3, n-3) acid, respectively.[20,21] Mammals cannot synthesize these PUFA, which, therefore, must be obtained from food or supplements. PUFA are mainly esterified into phospholipid cell membranes and are abundant in the brain. The release of PUFA from cell membranes or their variety of bioactive derivatives affect multiple brain processes, including cell survival, neurogenesis, neurotransmission, synaptic function, and neuroinflammation, thereby regulating mood and cognition.[22] The alteration of PUFA levels and their signaling pathways has been described in various neurological disorders, including AD and major depression.[23,24] Therefore, an adequate supply of dietary PUFA is considered important for neural health and brain disease prevention. Dietary PUFA is also essential in the kidney for such biological functions as mediating of renal prostaglandin production rearrangement, decreasing the production of pro-inflammatory leukotrienes, maintaining endothelial function, and controlling the escape rate of albumin across capillaries.[25] Diets containing PUFA conferred renoprotection in rats with immune- and/or inflammatory-mediated renal disorders,[26] and an n-3 FA metabolite could reduce kidney fibrosis in a murine model.[27]

Indeed, PUFA, sulfatides, and other sulfated glycans play critical roles in the brain and kidney. Although several studies have described the effects of PUFA on many types of brain and kidney diseases, the impact of PUFA on the metabolism of sulfated lysosomal substrates, such as sulfatides and other sulfated glycans, remains unknown. We hypothesized that changes in FA composition might affect the intracellular generation or degradation systems of these sulfated lysosomal substrates and possibly lead to a variety of diseases. This study investigated the effects of deficiency and supplementation of PUFA on the metabolism of sulfatides and sulfated GAGs in the brain and kidney.

2 | METHODS

2.1 | Animals and treatments

All animal experiments were performed in accordance with animal study protocols approved by the Shinshu University School of Medicine (approval number: 270044). Seven- to 8-week-old male C57BL/6 strain mice were obtained from

Charles River Laboratories Japan (Yokohama, Japan) and maintained in a controlled environment (22-23°C; 12 hours light/dark cycle) with 5% (w/w) crude fat-containing standard rodent chow (MF; Oriental Yeast, Tokyo, Japan) and water ad libitum. After a 1-week acclimatization period, the mice were randomly divided into control, PUFA (+), and PUFA (−) groups. The 0-week control group (n = 3), 5-week control group (n = 4), and 8-week control group (n = 4) were continuously fed the standard diet. The other groups were switched to a 14% (w/w) hydrogenated coconut oil (HCO)-containing PUFA-deficient diet (AIN-93G based; Oriental Yeast) for 2, 5, and 8 weeks (n = 4 for each period) to evaluate the time course of sulfatide expression. The FA composition of the HCO-containing PUFA-deficient diet was investigated in our past study to be as follows: C6:0, 0.2%; C8:0, 2.6%; C10:0, 6.4%; C12:0, 63.3%; C14:0, 15.7%; C16:0, 5.3%; and C18:0, 6.5% in total FA.[28] The detailed nutritional composition of this diet is shown in Table S1. In general, two types of PUFA-deficient diets have been used in past studies: a 4%-5% (w/w) HCO-containing diet and a fat-free diet. However, these diets may cause long-chain FA-insufficient intake, which can exert considerable effects in addition to those of a PUFA deficiency. To mitigate the influence of a long-chain FA deficiency on experiments, we employed the 14% (w/w) HCO-containing diet that contained long-chain FA at a standard level (4% in diet, w/w).[28]

From the 1st day of the PUFA-deficient diet feeding period, the PUFA (+) group was orally treated with n-3/n-6-balanced PUFA-containing oil (soybean oil [product number: 190-03776] plus linseed oil [product number: 125-01046] mixed at 1:1, v/v) at 0.2 mL/mouse every other day (typically at 7 PM) at a physiological level. In order to ensure the same calorie intake in both test groups, the PUFA (−) group was orally treated with PUFA-deficient oil (coconut oil [product number: 036-20905]) by the same method. All oils were purchased from Wako Pure Chemical Industries (Osaka, Japan). The soybean and linseed oils were mixed at 1:1 and aliquoted. The coconut oil was immediately aliquoted. The FA compositions of these oils are shown in Table S2. All oil aliquots were stored at −25°C and thawed at 37°C for 3 minutes before administration. After the experimental period determined for each group, the mice were anesthetized by isoflurane (Wako) inhalation followed by immediate brain and kidney collection and storage at −75°C until analysis.

2.2 | Quantitative and qualitative analyses of sulfatides

After weighing each brain or kidney sample, specimens were homogenized in four volumes of cold water. Sulfatides were extracted from 50 μL of tissue homogenate obtained from each mouse according to the hexane/isopropanol method.[29] Aliquots of 50 μL of standard human serum sample with an established sulfatide concentration were used as the standard for quantification of sulfatide concentration of test samples. The samples were then converted to lysosulfatides (LS; sulfatides without fatty acids) by saponification with sodium hydroxide.[30] The LS samples were purified by Mono-tip C18 cartridges (GL Sciences, Tokyo, Japan) followed by the addition of *N*-acetyl LS possessing sphinganine (LS-d18:0) as the calibrator. The samples were analyzed by matrix-assisted laser desorption ionization-time of flight mass spectrometry (MALDI-TOF MS) on a TOF/TOF 5800 system (AB Sciex, Framingham, MA, USA) in negative ion reflector mode with two-point external calibration using *N*-acetylated LS-d18:0 ($[M–H]^-$ 584.310) and LS-(4E)-sphingenine (d18:1) ($[M–H]^-$ 540.284) peaks. We employed 9-aminoacridine as the matrix for MALDI-TOF MS.[31,32] Based on the differences in sphingoid base structure, the following molecular species of LS were detected: LS-sphingadienine (d18:2), LS-d18:1, LS-d18:0, LS-phytosphingosine (t18:0), LS-(4*E*)-icosasphingenine (d20:1), LS-icosasphinganine (d20:0), and LS-4D-hydroxyicosasphinganine (t20:0). The sum of these seven LS species was calculated as the total sulfatide level in a sample (μmol/g wet tissue weight).

2.3 | qPCR analysis

Total RNA was isolated from brain and kidney samples using an RNeasy Mini kit (QIAGEN, Hilden, Germany) and reverse transcribed using a PrimeScript RT Reagent kit (Takara Bio, Otsu, Japan). The gene expression of related mRNA was measured by the quantitative real-time polymerase chain reaction (qPCR) with SYBR Premix Ex Taq II (Takara Bio) on a Step One Plus (Thermo Fisher Scientific, Rockford, IL, USA). The gene-specific primers listed in Table 1 were designed using Primer Express software (Applied Biosystems, Waltham, MA, USA). Data analysis were carried out using the $\Delta\Delta C_t$ method, normalized to GAPDH gene levels, and presented as fold changes with the value of the control mice as 1.

2.4 | Immunoblot analysis

The preparation of whole-tissue lysates (brain and kidney) and immunoblot analysis were conducted as described previously.[32,33] The primary antibodies used for immunoblot testing included anti-β-actin (1:1000), anti-cerebroside sulfotransferase (CST) (1:2000), anti-ceramide galactosyltransferase (CGT) (1:2000), anti-arylsulfatase A (ARSA) (1:2000), anti-mammalian target of rapamycin (mTOR) (1:1000), anti-phospho-mTOR (S2448) (1:1000), anti-AKT (1:4000), and anti-amyloid precursor protein (APP) (1:5000)

TABLE 1 Primer pairs used for qPCR

Gene	Gene bank accession number	Primer sequence (5′ to 3′)
CST	NM_016922	F ATGGCCTTCACGACCTCAGA
		R CGGTCTTGTGCGTCTTCATG
CGT	NM_011674	F TGGGTCCAGCCTATGGATGT
		R GCAGCGTTGGTCTTGGAAAC
ARSA	NM_009713	F ACCACCCCTAACCTGGATCAGT
		R ATGGCGTGCACAGAGACACA
GALC	NM_008079	F GAGTGAGAATCATAGCGAGCGATA
		R AGTTCCTGGTCCAGCAGCAA
GAPDH	M32599	F TGCACCACCAACTGCTTAG
		R GGATGCAGGGATGATGTTCTG

Abbreviations: F, forward sequence; R, reverse sequence.

(Abcam, Cambridge, UK); anti-galactosylceramidase (GALC) (1:1000) (Proteintech, Chicago, IL, USA); anti-p62 (1:1000), anti-Beclin1 (1:1000), and anti-Atg5 (1:500) (Medical & Biological Laboratories, Co., Ltd., Nagoya, Japan); anti-microtubule associated protein 1 light chain 3B (LC3B) (1:500) (Novus Biologicals, Centennial, CO, USA); anti-P53 (1:500) (Santa Cruz Biotechnology, Dallas, TX, USA); anti-extracellular regulated protein kinase-1/2 (Erk1/2) (1:1000) (Upstate Cell Signaling Solution, Lake Placid, NY, USA); anti-phospho-Erk1/2 (1:2000), anti-AMP-activated protein kinase α (AMPKα) (1:1000), anti-phospho-AMPKα (1:1000), and anti-phospho-AKT (1:1000) (Cell Signaling Technology, Danvers, MA, USA); and anti-*β*-glucuronidase (1:500)[34] that was kindly provided by Dr K. Sukegawa from Gifu University School of Medicine, Gifu, Japan. After incubation with the primary antibodies, the membranes were subjected to horse radish peroxidase secondary antibodies and then, treated with ECL Prime Western Blotting Detection Reagent (GE Healthcare, Little Chalfont, UK). Band intensities were measured densitometrically using an ECL Imager (Thermo Fisher Scientific), compared with that of *β*-actin, and subsequently expressed as fold changes relative to those of the control mice.

2.5 | Transmission electron microscopy

Tissues used for transmission electron microscopy were obtained from the brain stem or renal cortex. The samples were sliced into small cubes of approximately 1 mm^3 and then, immediately fixed in 2.5% glutaraldehyde and postfixed with 1.5% osmium tetroxide. Dehydration was performed in a graduated ethanol series, followed next by embedding in Epon resin. Ultrathin sections were doubly stained with uranyl acetate and lead citrate and analyzed at 80 kV on a JEM 1400 electron microscope (JEOL, Tokyo, Japan).[35,36]

2.6 | Immunofluorescence staining analysis

Brain and kidney cryosections of 6 μm thickness were rinsed three times with phosphate buffer solution (PBS) followed by permeabilization with 0.3% Triton X-100 in PBS for 30 minutes at room temperature. After blocking with 4% bovine serum albumin (BSA) for 60 minutes, the slides were immunostained overnight at 4°C with antibodies against lysosome associated membrane protein type 1 (LAMP-1) (1:100 dilution; mouse monoclonal) (American Research Products), LC3B (1:100 dilution; rabbit monoclonal), and β-amyloid (1-42 Preferred) (1:1000 dilution; rabbit monoclonal) that were diluted in 1% BSA in 0.1% Triton X-100/PBS. After rinsing three times with PBS, the samples were incubated at room temperature for 1 hour with FITC- and Cy3-conjugated secondary antibodies (Jackson ImmunoResearch, West Grove, PA, USA). Subsequent to washing with PBS, the samples were stained with 4′, 6-diamidino-2-phenylindole to visualize the nuclei and then, mounted using a fluorescence mounting medium (Agilent, Santa Clara, CA, USA). Slides were observed on a Zeiss LSM880 confocal imaging system (Fluoview; Olympus, Tokyo, Japan).

2.7 | Immunohistochemical analysis

Fresh tissue slices of mouse brain and kidney were embedded in Tissue-Tek OCT compound (Sakura Finetek, Tokyo, Japan) and frozen at −80°C. The samples were sectioned at 6 μm of thickness, air-dried, and fixed with 10% neutral buffered formalin (pH 7.4) for 5 minutes. After rinsing with running water, the tissue slides were treated using a 0.3% hydrogen peroxide solution for 10 minutes to block endogenous peroxidase activity. After being rinsed in 50 mM Tris-buffered saline (TBS) (pH 7.6) three times, the slides were immunostained using a Histofine Mousestain Kit

(Nichirei Biosciences, Tokyo, Japan). A primary antibody against chondroitin sulfate-A (CS-A) (clone 2H6; mouse IgM) (Seikagaku Co., Tokyo, Japan) was applied for 1 hour at room temperature as earlier described,[37] and peroxidase activity was developed using a 3, 3′-diaminobenzidine/hydrogen peroxide solution for 15 minutes. A negative control experiment was conducted by omitting the primary antibody from the staining procedure. Slides were observed on a Zeiss AxioObserverZ1 imaging system (Fluoview; Olympus, Tokyo, Japan).

2.8 | GAG extraction and quantification

Sulfated GAGs in the brain and kidney were extracted, and their contents were quantified according to the instructions of the Blyscan Sulfated Glycosaminoglycan Assay (Biocolor Ltd., County Antrim, BT38 8YF, UK). First, the papain extraction reagent was prepared: 5 mg of papain (Sigma-Aldrich, St. Louis, MO, USA) was added to 50 mL of a 0.2 M sodium phosphate buffer (pH 6.4) containing 400 mg sodium acetate, 200 mg EDTA disodium salt, and 40 mg cysteine HCl. Samples of 20 mg of brain or kidney tissue received 1 mL of papain extraction reagent and were digested at 65°C for 3 hours. Samples were centrifuged at 10 000 *g* for 10 minutes, and supernatants were used for the measurement of total sulfated GAGs. Part of the supernatant was also used for the differentiation of N-sulfated and O-sulfated GAGs by the nitrous acid cleavage method. The extracted GAG samples were mixed with the same volume of a sodium nitrite reagent and 33% acetic acid solution. The reaction was allowed to proceed for 60 minutes at room temperature with occasional mixing. After the reaction, an equal volume of ammonium sulfamate reagent was added and mixed over a period of 10 minutes. At this time, the sample was an O-sulfated glycosaminoglycan extract for measurement. Total sulfated GAG and O-sulfated GAG levels were measured using the Blyscan protocol. O-sulfated GAG levels were subtracted from total sulfated GAG levels to determine the levels of N-sulfated GAGs. Hyaluronan (HA) is a non-sulfated GAG and cannot be detected by this assay.

2.9 | Statistical analysis

All data examined are presented as the mean ± standard deviation. Statistical analysis of the differences between groups was performed by ANOVA followed by Tukey's post hoc test. Differences in time-course changes were evaluated using the unpaired Student's *t* test by SPSS software v26J (IBM, New York, NY, USA). A P value of $<.05$ was considered statistically significant.

3 | RESULTS

3.1 | A PUFA-deficient diet significantly decreased the expression level of brain sulfatides by increasing sulfatide degradative enzyme proteins without mRNA change

During the experimental period, there were no remarkable differences in food intake among the groups, with all mice surviving and exhibiting no neurological abnormalities. There were no significant changes in body or organ weight between the PUFA (+) and PUFA (−) groups at any time point (Table 2).

To investigate whether a PUFA deficiency affected metabolism among sulfated lysosomal substrates, we first examined the time-course changes in the content of representative sulfated substrates, sulfatides, in the brain of mice. Whereas the brain sulfatide content in the PUFA (+) group was maintained, that in the PUFA (−) group was significantly decreased at 5 and 8 weeks (Figure 1A). These findings indicated that a PUFA-deficient diet reduced brain sulfatide content, which was prevented by PUFA supplementation.

Since brain sulfatide levels were stable from 5 weeks, we used the 5-week group of mice for the ensuing analyses. To investigate the mechanism underlying the decrease in brain sulfatide content in the PUFA (−) group, the protein and gene expression levels of sulfatide metabolic enzymes were examined next. The PUFA-deficient diet caused significant increases in ARSA and GALC, both major sulfatide degradative lysosomal enzymes, among protein expression levels, which was prevented by PUFA supplementation. Interestingly, the gene expression levels of ARSA and GALC did not differ among the groups (Figure 1B). The protein and gene expression levels of the sulfatide synthesis enzymes CST and CGT were comparable among the groups. These findings suggested that increases in ARSA and GALC proteins caused the degradation of brain sulfatides.

3.2 | A PUFA-deficient diet activated autophagy and lysosomal function in the brain stem

Lysosomes are known to play pivotal roles in the catabolic and anabolic responses to a variety of factors, including nutrient availability. Since a PUFA-deficient diet might create a starvation state of essential PUFA nutrients, we hypothesized that an inadequate availability of PUFA could lead to autophagy acting as a starvation response, and then, a large number of autophagosomes could fuse with lysosomes to activate lysosomal enzymes. To investigate this notion, we examined the brain expression levels of the autophagy marker LC3B, autophagy-related proteins Beclin1 and Atg5,

TABLE 2 Physiological data

	Control	2w HCO		5w HCO		8w	8w HCO	
		PUFA (+)	PUFA (−)	PUFA (+)	PUFA (−)	Control	PUFA (+)	PUFA (−)
Body weight (g)	25.57 ± 0.40	25.15 ± 0.79	24.35 ± 0.34	27.78 ± 0.29	26.60 ± 1.69	28.25 ± 1.18	27.53 ± 0.30	27.67 ± 0.59
Body weight change (%)	nd	100.25 ± 2.62	97.13 ± 4.08	110.81 ± 5.32	106.01 ± 6.08	112.55 ± 1.34	109.89 ± 4.06	110.39 ± 6.86
Brain/body weight (%)	1.79 ± 0.02	1.80 ± 0.06	1.81 ± 0.05	1.71 ± 0.06	1.71 ± 0.09	1.64 ± 0.02	1.68 ± 0.04	1.65 ± 0.03
Kidney/body weight (%)	1.38 ± 0.08	1.42 ± 0.10	1.40 ± 0.04	1.35 ± 0.07	1.26 ± 0.11	1.36 ± 0.12	1.40 ± 0.07	1.38 ± 0.07
Liver/body weight (%)	4.56 ± 0.02	4.28 ± 0.53	4.14 ± 0.19	4.35 ± 0.63	4.55 ± 0.3	4.30 ± 0.30	3.94 ± 0.27	4.20 ± 0.81

Note: Test mice were fed a 14% HCO-containing PUFA-deficient diet for 2, 5, or 8 weeks (2w, 5w, or 8w HCO). The control group was fed 5% (w/w) crude fat-containing standard rodent chow for comparisons. Data are shown as the mean ± SD (n = 3-4). There were no significant differences between the PUFA (+) and PUFA (−) groups at any time point.

Abbreviation: nd, not determined.

autophagy substrate P62, and a representative lysosomal enzyme, β-glucuronidase, by immunoblot analysis (Figure 2A). Compared with PUFA (+) mice, the protein expression levels of LC3B, Beclin1, Atg5, and β-glucuronidase were remarkably increased, and that of P62 was decreased, in the brain of PUFA (−) mice.

To further verify the relationship between autophagy and lysosomes, the co-localization of LC3B with LAMP-1, a representative lysosomal marker, was examined by double immunofluorescence staining analysis (Figure 2B). Double staining revealed expression and co-localization of LC3B with LAMP-1 in the brain stem of PUFA (−) mice, which were absent in the PUFA (+) group.

Brain stem samples in each group were examined by transmission electron microscopy to confirm the activation of autophagy. In the PUFA (−) group, the number of autolysosomes clearly enclosing recognizable specific organelles or organelle fragments was significantly increased compared with the PUFA (+) group (Figure 2C). Moreover, magnified images of PUFA (−) mice distinctly showed the classical structures of autolysosomes (Figure 2D).

Since autophagy is most obvious in the brain stem, we examined the expression levels of sulfatides and the lysosomal enzymes ARSA, GALC, and β-glucuronidase for brain stem samples only. These confirmation experiments demonstrated significant degradation of sulfatides and elevated protein expression of lysosomal enzymes in the brain stem (Figure S1).

3.3 | Time-course changes in protein expression levels of ARSA and LC3B in the brain

In order to better characterize the relationship between autophagy and sulfatide degradation, we investigated the time-course changes in protein expression of the lysosomal enzyme ARSA and autophagy marker LC3B using the brain of mice treated for 0, 2, 5, and 8 weeks. ARSA and LC3B were significantly increased from the 5th week to the 8th week in the PUFA (−) group, with no remarkable changes in the PUFA (+) group (Figure 3). These findings suggested that a PUFA-deficient diet activated autophagy to thereby, enhance the lysosomal enzyme function, which might be associated with sulfatide degradation in the brain stem, all of which were attenuated by PUFA supplementation.

3.4 | A PUFA-deficient diet-induced autophagy by suppressing the Erk/mTOR signaling pathway

The canonical autophagy pathway characterized by the biogenesis of membrane structures is regulated by mTOR

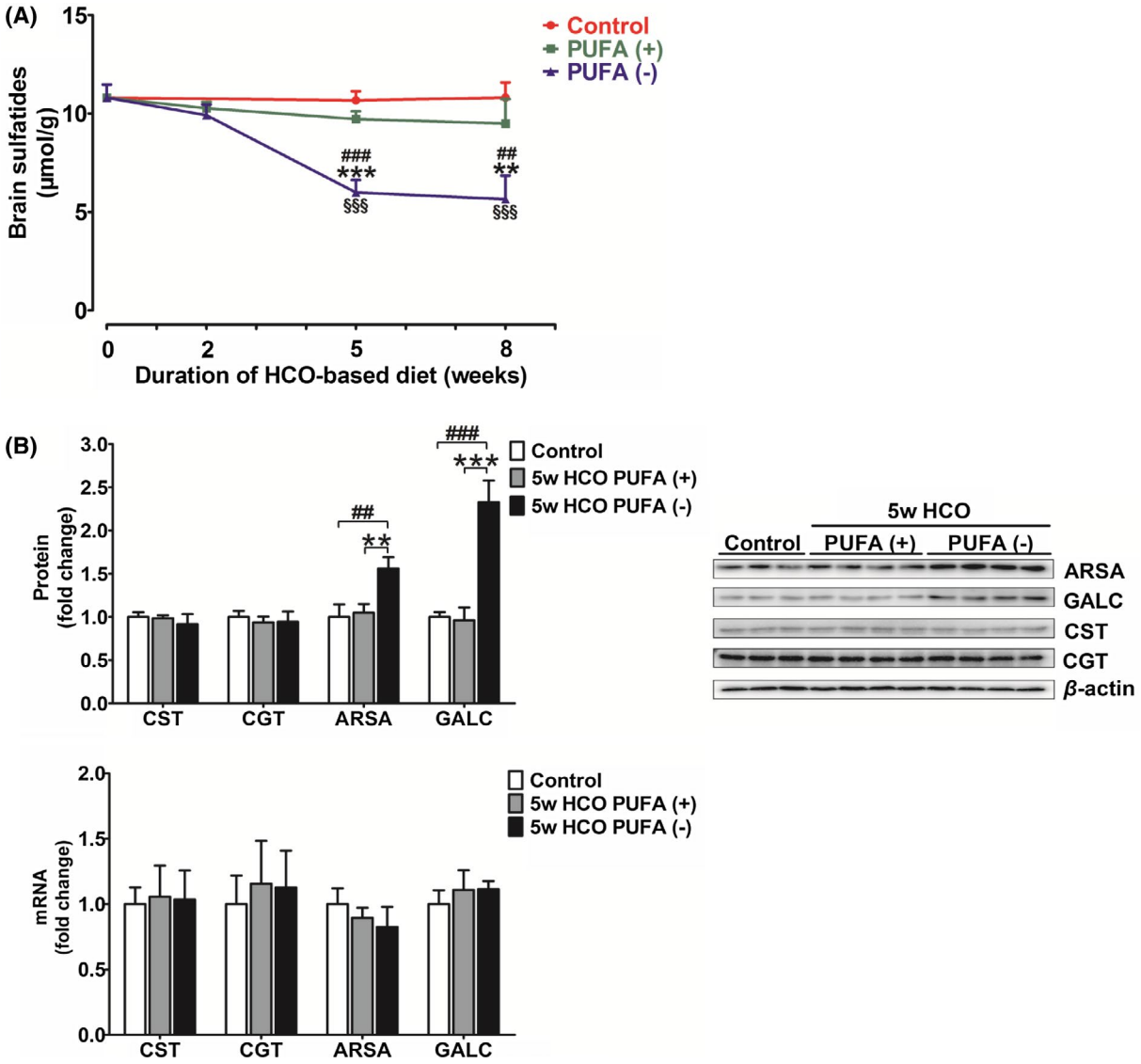

FIGURE 1 Changes in sulfatide levels and the expression of sulfatide metabolic enzymes in the brain of mice. A, Sulfatide levels in the brain were measured by MALDI-TOF MS. The total amount of sulfatides was calculated as the sum of seven lysosulfatide molecular species (μmol/g wet brain weight). PUFA (+), group supplemented with PUFA-containing oil; PUFA (−), group supplemented with PUFA-deficient oil. Data are expressed as the mean ± SD (n = 3-4). *P* values comparing each time point with control mice of 0 weeks were calculated by the unpaired Student's *t* test: $^{§§§}P < .001$. Differences between groups were compared using ANOVA with Tukey's *post hoc* test: $^{**}P < .01$, $^{***}P < .001$ vs PUFA (+) group; $^{##}P < .01$, $^{###}P < .001$ vs control group. B, Immunoblot and gray analyses showing the expressions of protein levels of sulfatide-synthesizing enzymes (CST and CGT) and sulfatide-degrading enzymes (ARSA and GALC). 5w HCO: mice fed a 14% HCO-based diet for 5 weeks. Protein levels were normalized to that of *β*-actin. Analysis of mRNA levels of these enzymes were performed by real-time PCR and normalized to that of GAPDH. All data are shown as fold changes relative to the control group. Data are expressed as the mean ± SD (n = 3-4). Statistically significant differences: $^{**}P < .01$, $^{***}P < .001$ vs PUFA (+) group; $^{##}P < .01$, $^{###}P < .001$ vs control group

complex 1.[38] It has been reported that autophagy can be activated by the suppressive effects of p53 and AMPK on mTOR.[39,40] Therefore, we investigated whether p53, AMPKα phosphorylation, and mTOR phosphorylation were involved in the autophagy induced by a PUFA-deficient diet. As shown in Figure 4, a PUFA insufficiency resulted in the remarkable inhibition of p-mTOR (S2448), but had no obvious effect on p-AMPKα or p53. Since AKT or the mitogen-activated protein kinase (MAPK)/Erk1/2 signaling cascade upstream of mTOR are the main regulatory pathways to suppress autophagy.[41-43] Erk1/2 and AKT phosphorylation were examined next. While a PUFA-deficient diet reduced phosphorylation levels of Erk1/2, it did not alter p-AKT levels. These findings implicated the Erk/mTOR pathway as the main signaling cascade for the induction of autophagy by a PUFA-deficient diet.

3.5 | A PUFA-deficient diet decreased the protein expression levels of amyloid precursor proteins in the brain

Autophagy disorders play prominent roles in amyloid β (Aβ) metabolism and are extensively involved in AD pathogenesis.[44] The decrease of sulfatides is also tightly associated with deterioration of Aβ clearance.[45] To investigate whether PUFA deficiency-induced autophagy activation and the related sulfatide degradation were associated with the pathogenesis of AD, we evaluated the protein expression of APP and Aβ deposition in the brain of PUFA-deficient mice. Although no Aβ deposition was detected (Figure 5B), a significant decrease in APP appeared at 8 weeks in the PUFA (−) group (Figure 5A). These results indicated that PUFA deficiency-induced autophagy activation and sulfatide degradation might be involved in the early developmental process of AD.

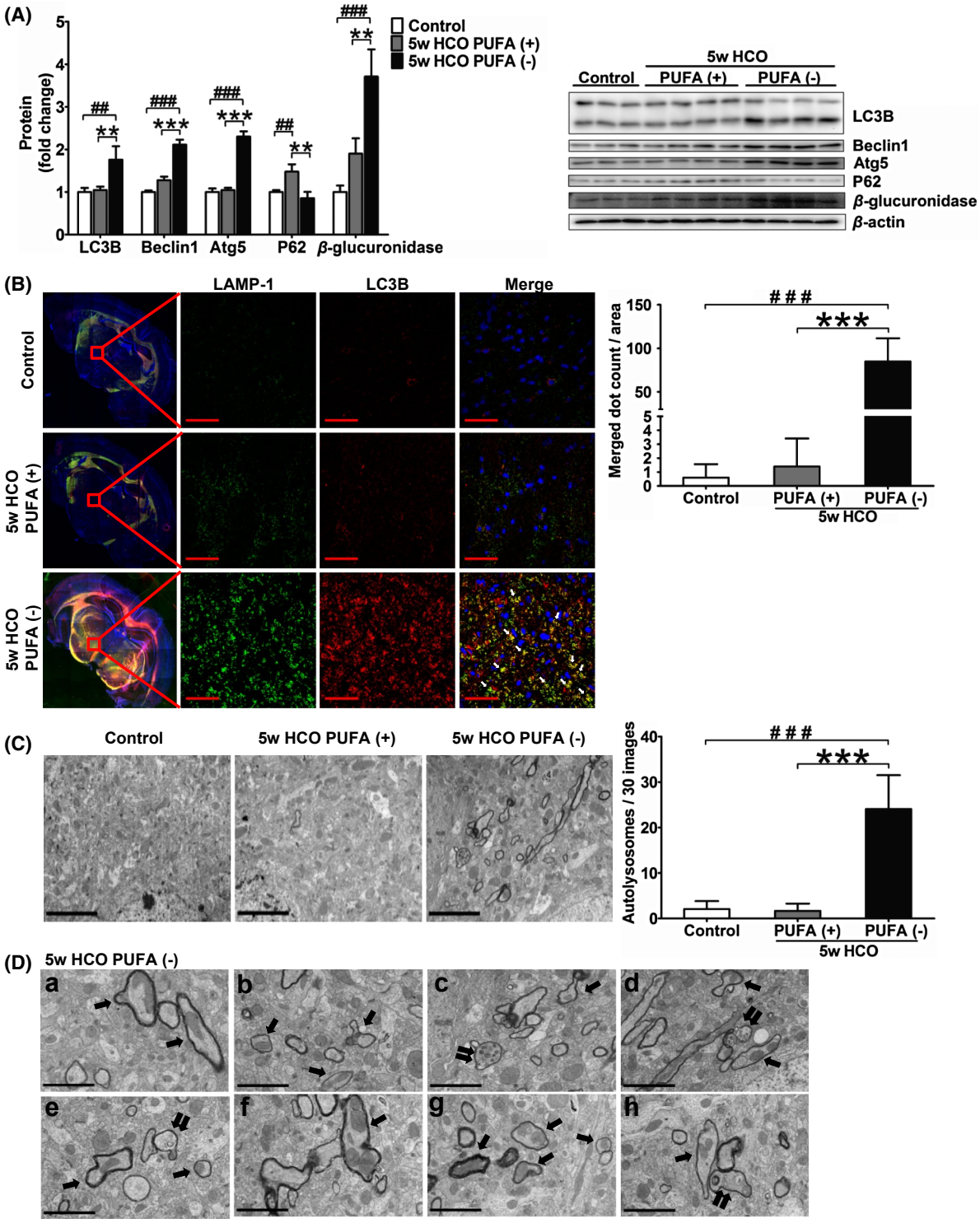

FIGURE 2 A PUFA-deficient diet activates autophagy and lysosomal function in the brain stem of mice. A, Immunoblot and gray analyses of the autophagy markers LC3B, Beclin1, and Atg5, the autophagy substrate P62, and a representative lysosomal enzyme, β-glucuronidase. Protein levels were normalized to that of β-actin. All data are shown as fold changes relative to control mice. B, Co-localization of the autophagy marker LC3B with LAMP-1 in the brain. Confocal images of brain samples obtained from mice of each group. LC3B was stained using a Cy3-conjugated IgG secondary antibody (red) and LAMP-1 was visualized with a FITC-conjugated secondary antibody (green), followed by counterstaining with DAPI (blue). Arrows indicate the co-localization of LC3B and LAMP-1. Scale bar represents 50 μm. Left panels demonstrate whole-tissue immunofluorescence staining. The number of LC3B + LAMP-1 merged dots was counted in at least 10 high-power fields in control, 5w HCO PUFA (+), and 5w HCO PUFA (−) brains. C, Representative electron micrographs of each group. The number of autolysosomes counted in at least 30 images of PUFA (+) and PUFA (−) mice were compared. Scale bar represents 5 μm. D, Classical autophagic structures in the PUFA (−) group. a-h: Single arrows identify autolysosomes that are clearly enclosing organelle fragments or recognizable organelles, such as mitochondria. Double arrows indicate autolysosomes with organelles in varying states of degradation. Scale bar represents 2.5 μm. All data are expressed as the mean ± SD. Statistically significant differences by ANOVA with Tukey's *post hoc* test: $^{**}P < .01$, $^{***}P < .001$ vs PUFA (+) group; $^{\#\#}P < .01$, $^{\#\#\#}P < .001$ vs control group

3.6 | Effects of a PUFA-deficient diet on another sulfatide-rich organ, the kidney

We examined another sulfatide-rich organ, the kidney, to determine whether sulfatide degradation and autophagy activation caused by a PUFA deficiency occurred systemically. As in the brain, a PUFA-deficient diet decreased the expression level of sulfatides in the kidney from 5 to 8 weeks (Figure 6A). The renal protein levels of ARSA and GALC were increased remarkably without alterations in gene levels in the 5-week-fed PUFA (−) group (Figure 6B). Furthermore, the protein levels of LC3B, Beclin1, Atg5, and β-glucuronidase were increased, with a decreasing trend of P62, at 5 weeks in PUFA (−) mice (Figure 6C). The above changes in sulfatide metabolic enzymes and autophagy-related proteins in the kidney exhibited remarkably similar patterns to those in the brain.

3.7 | A PUFA-deficient diet activated autophagy and lysosomal function in the kidney cortex

To verify whether lysosomal hyperfunction was associated with autophagy in the kidney, immunofluorescence examining the co-localization of LAMP-1 and LC3B and transmission electron microscopy were conducted. As expected, immunofluorescence analysis showed higher expression and co-localization of LAMP-1 and LC3B in the renal cortex of the 5-week-fed PUFA (−) group (Figure 7A). Transmission electron microscopy analysis also demonstrated an increase in autolysosomes and detected various classical autophagic structures at 5 weeks in PUFA (−) mice (Figure 7B). Confirmation analyses using kidney cortex samples demonstrated a significant decrease in sulfatide levels and increase in the protein expression of the lysosomal enzymes ARSA, GALC, and β-glucuronidase (Figure S2). These results corresponded with those using whole kidney samples. Furthermore, significant decreases in the expressions of p-mTOR and p-Erk1/2 were detected in the kidney of the PUFA (−) group (Figure 7C).

3.8 | Time-course changes in protein expression levels of ARSA and LC3B in the kidney

The time-course changes in the protein expression levels of ARSA and LC3B were examined using the kidney of mice treated for 0, 2, 5, and 8 weeks. ARSA and LC3B protein expression were significantly increased from the 5th week to the 8th week in the PUFA (−) group (Figure 8).

The cumulative kidney findings indicated that changes in sulfatide degradation, autophagy activation, and lysosome hyperfunction caused by a PUFA deficiency occurred systemically, likely by means of the same mechanism as in the brain.

3.9 | A PUFA-deficient diet significantly reduced other representative lysosomal enzyme substrates, GAGs, in the brain and kidney

From the above results, we speculated that a PUFA deficiency might promote general lysosomal function associated with autophagy activation. The significantly increased β-glucuronidase in this study is a representative lysosomal enzyme that plays a vital role in the normal step-wise degradation of GAGs.[46] We hypothesized that the lysosomal hyperfunction caused by a PUFA deficiency was not specific to sulfatide metabolism, so we examined the expression changes of other typical lysosomal enzyme substrates, that is, GAGs, in the brain and kidney. GAGs are polysaccharides composed of repeating disaccharide units that are classified into five classes: chondroitin sulfate (CS), heparan sulfate/heparin (HS), keratan sulfate (KS), dermatan sulfate (DS), and HA.[15] HS contains both N-sulfated and O-sulfated hexosamines, whereas the other sulfated GAGs, CS, KS, and DS,

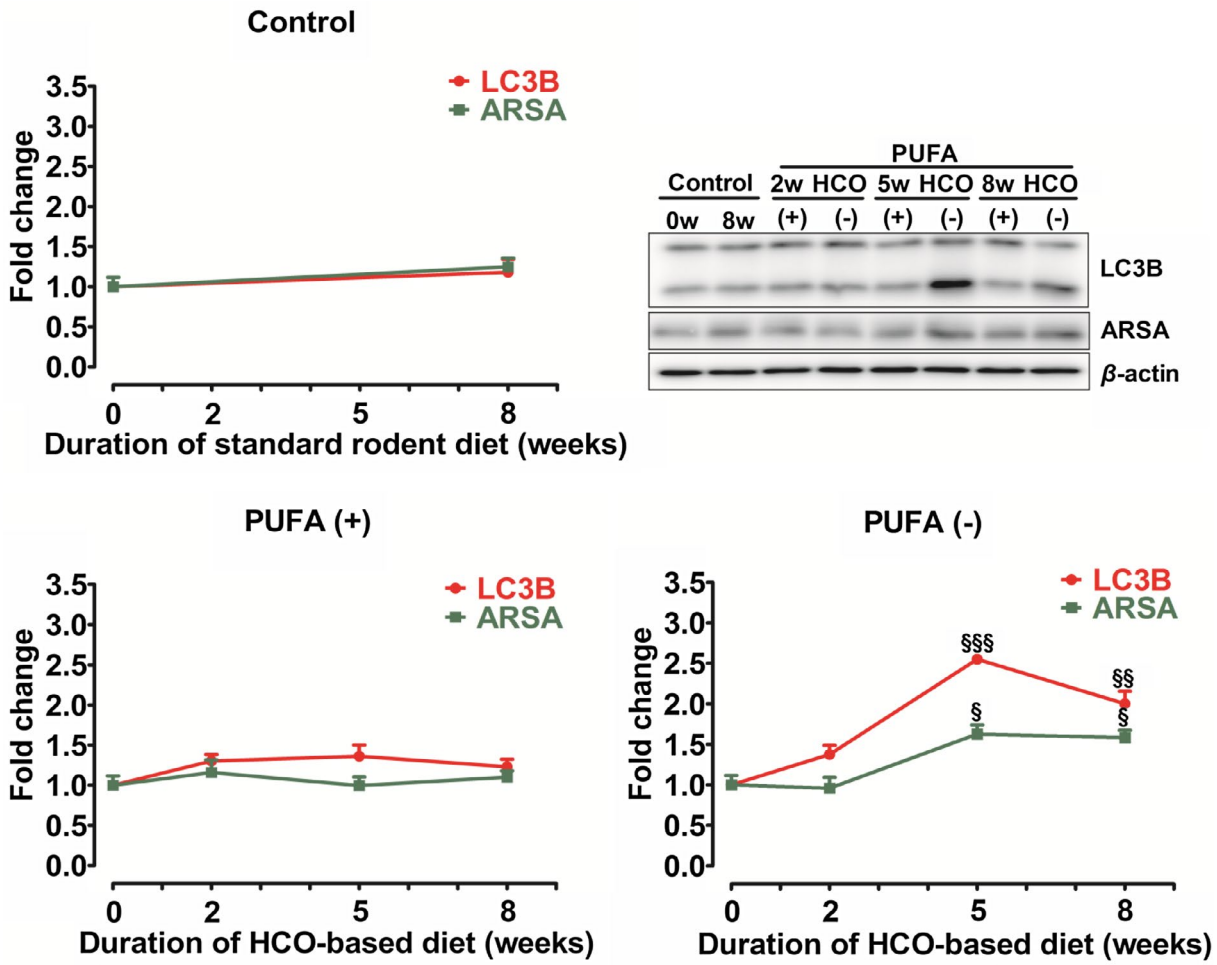

FIGURE 3 Time-course changes in expression levels of ARSA and LC3B in the brain of mice. The protein expression levels of ARSA and LC3B were examined by immunoblot and gray analyses. Protein levels were normalized to that of β-actin. All data are shown as fold changes relative to the control group at 0 weeks. Data are expressed as the mean ± SD (n = 3-4). *P* values comparing each time point with control mice of 0 weeks were calculated by the unpaired Student's *t* test: $^{\S}P < .05$, $^{\S\S}P < .01$, $^{\S\S\S}P < .001$

contain O-sulfated hexosamines only. HA is a non-sulfated GAG. The experiment using the sulfated GAG measuring assay kit revealed a significant decrease in total sulfated GAGs, mainly via O-sulfated GAG reduction, in the brain and kidney of the 5-week PUFA (−) group (Figure 9A). To investigate the localization of sulfated GAG changes, we performed an immunohistochemical analysis on CS-A, a representative O-sulfated GAG. In brain tissue sections, CS-A expression was significantly decreased in the brain stem of the PUFA (−) group, which was consistent with autophagy and lysosomal activated lesions (Figure 9B). The same analysis was performed on kidney samples, but reliable results were unobtainable due to severe nonspecific staining (data not shown).

4 | DISCUSSION

Considerable evidence has shown that dietary n-6 and n-3 FA influence the composition and function of structural components in vivo. Our results demonstrated that a PUFA-deficient diet could reduce the expression of sulfatides and sulfated GAGs in both the brain and kidney of mice. Regarding the metabolic mechanism of this decrease, the current study is the first to reveal that a PUFA deficiency may stimulate autophagy and lysosomal enzyme function via suppression of the Erk/mTOR pathway; these may be associated with the degradation of sulfatides and sulfated GAGs. In the present study, time-course analyses indicated that a PUFA deficiency significantly decreased sulfatide levels in the brain and kidney for 2-5 weeks, after which levels were maintained. Our results in Figures 3 and 8 indicated that a PUFA deficiency-induced autophagy activation and lysosomal hyperfunction for 2-5 weeks. These activations appeared to reach a saturation level, and then, began to slightly decrease at the 8th week, thus mirroring the changes in sulfatide levels. Several past studies have demonstrated that the autophagy activation cannot continue to increase, and reach saturation and eventually weaken, even with continuous autophagy stimulation signals such as angiotensin II and

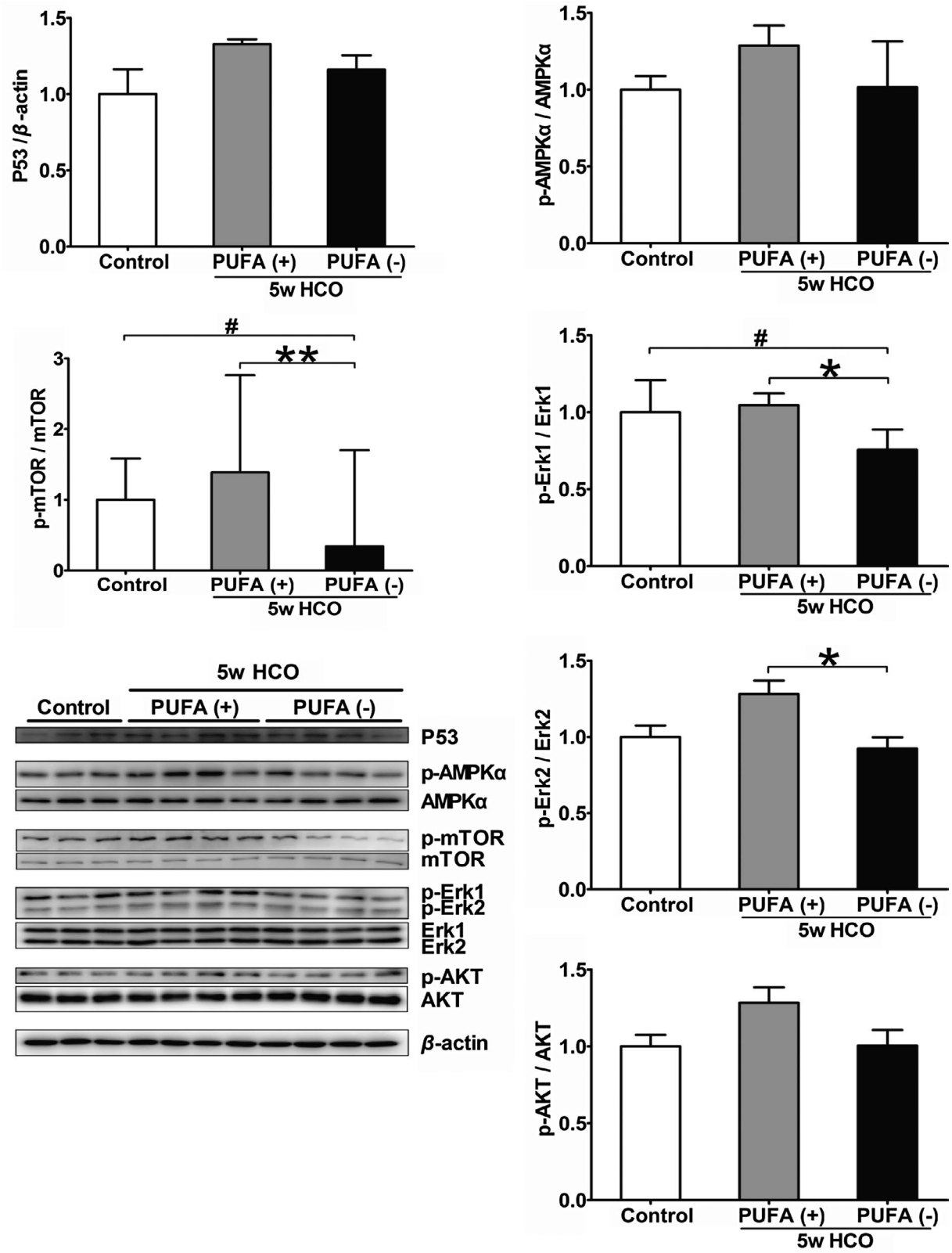

FIGURE 4 A PUFA-deficient diet induced autophagy via suppression of the Erk/mTOR pathway in the brain of mice. The protein expression of p53 and the relative ratios of total and phosphorylated protein levels of AMPKα, mTOR, Erk1/2, and AKT were examined by immunoblot and densitometric analyses. Data are expressed as the mean ± SD (n = 3-4). All data are shown as fold changes relative to the control group. Statistically significant differences by ANOVA with Tukey's *post hoc* test: $^{*}P < .05$, $^{**}P < .01$ vs PUFA (+) group; $^{\#}P < .05$ vs control group

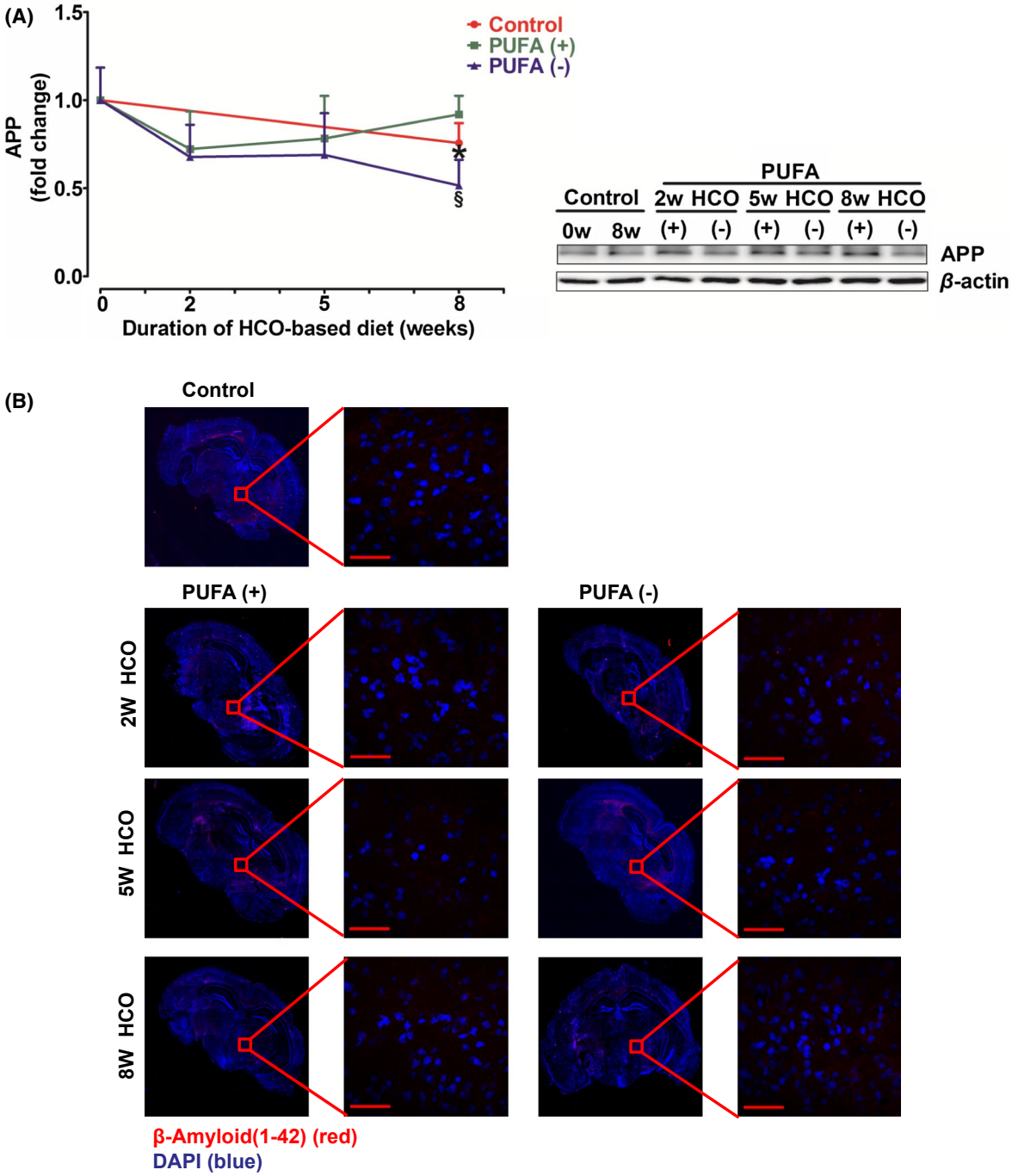

FIGURE 5 Time-course changes in the protein level of APP and immunofluorescence analysis of amyloid β in the brain of mice. A, The protein expression level of APP was examined by immunoblot and gray analyses. All data are shown as fold changes relative to the control group at 0 weeks. Data are expressed as the mean ± SD (n = 3-4). *P* values comparing each time point with control mice of 0 weeks were calculated by the unpaired Student's *t* test: $^{\S}P < .05$. Differences between groups were compared using ANOVA with Tukey's *post hoc* test: $^{*}P < .05$ vs PUFA (+) group. B, Confocal images of brain samples obtained from mice of each group. Samples were subjected to immunofluorescence for amyloid β (1-42) (red) and DAPI (blue). Left panels represent whole-tissue immunofluorescence staining. Scale bar represents 50 μm

H_2O_2.[47,48] The time-dependent changes in autophagy by continuous PUFA-deficient signals were consistent with those results. Moreover, the synchronized time-dependent changes observed in this study suggest a close relationship among the organ contents of sulfatides and sulfated GAGs, autophagy activation, and lysosomal hyperfunction.

The present study indicated that the sulfatide level decrease in the brain and kidney was caused by sulfatide degradation enhancement via increase in the lysosomal sulfatide degradative enzymes ARSA and GALC. In the induction process of these enzymes, we observed the interesting phenomenon of augmented protein expression of these enzymes without

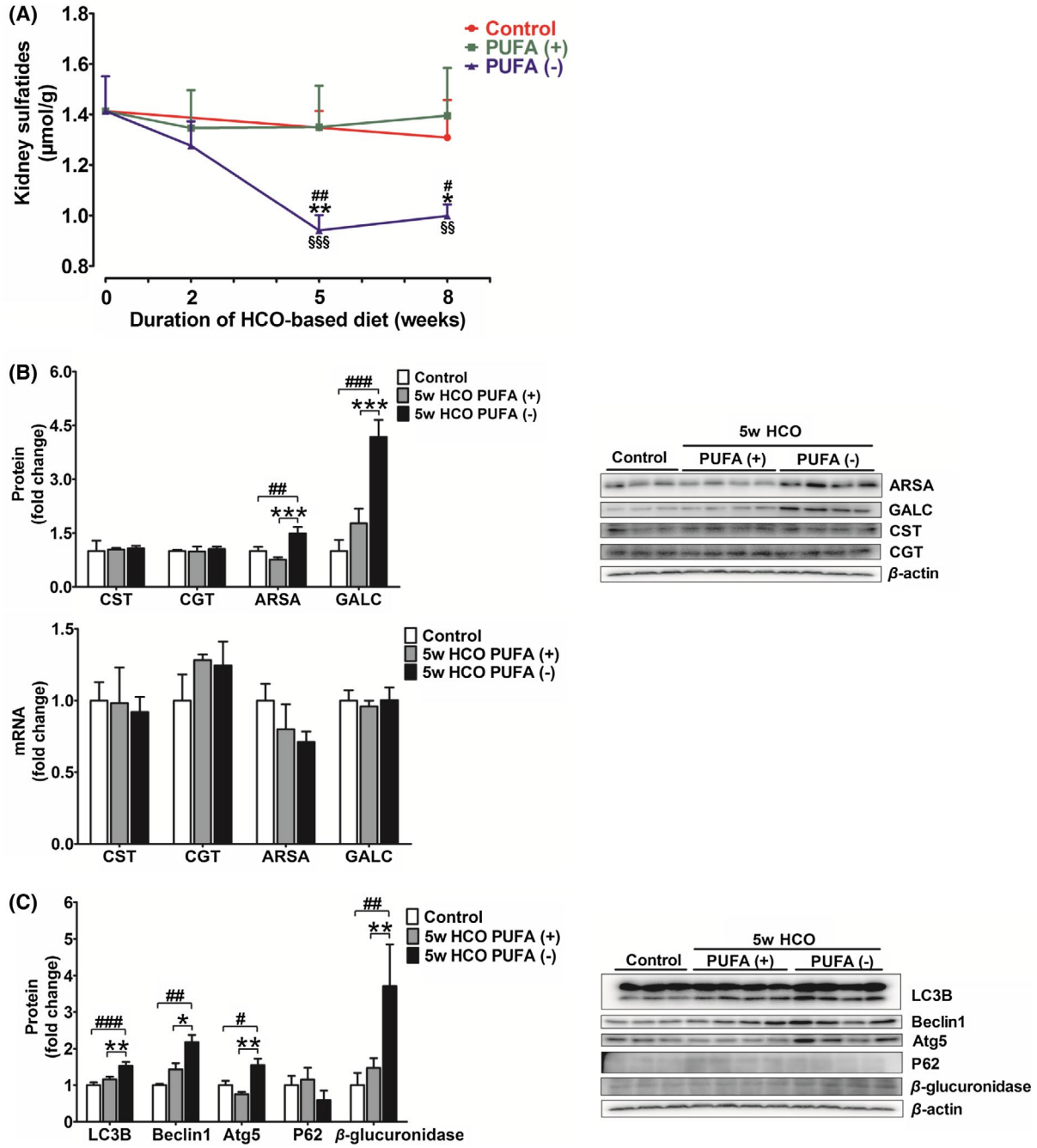

FIGURE 6 A PUFA deficiency diet caused sulfatide degradation and autophagy in the kidney. A, Time-course changes in the content of kidney sulfatides (μmol/g wet kidney weight). Data are expressed as the mean ± SD (n = 3-4). *P* values comparing each time point with control mice of 0 weeks were calculated by the unpaired Student's *t* test: $^{§§}P < .01$; $^{§§§}P < .001$. Differences between groups were compared using ANOVA with Tukey's *post hoc* test: $^{*}P < .05$, $^{**}P < .01$ vs PUFA (+) group; $^{\#}P < .05$, $^{\#\#}P < .01$ vs control group. B, Protein amounts and mRNA expression levels of sulfatide metabolic enzymes in the kidney of 5-week-fed mice. Protein levels were normalized to that of *β*-actin. Levels of mRNA were measured and normalized to that of GAPDH. C, Protein amounts of autophagy makers, substrates, and a representative lysosomal enzyme in the kidney of mice. Protein levels were normalized to that of *β*-actin. All data are shown as fold changes relative to the 0-week-fed control group and expressed as the mean ± SD (n = 3-4). Statistically significant differences by ANOVA with Tukey's *post hoc* test: $^{*}P < .05$, $^{**}P < .01$, $^{***}P < .001$ vs PUFA (+) group; $^{\#}P < .05$, $^{\#\#}P < .01$, $^{\#\#\#}P < .001$ vs control group

gene upregulation. In the general autophagy activation process, transcription factor EB (TFEB), a master regulator of lysosomal biogenesis and autophagy, is activated and binds coordinated lysosomal expression and regulation (CLEAR) DNA sequences to participate in transcriptional regulation, including autophagosome formation, autophagosome/lysosome fusion, and lysosomal biogenesis.[49,50] Therefore, it is possible that a PUFA deficiency may increase many types

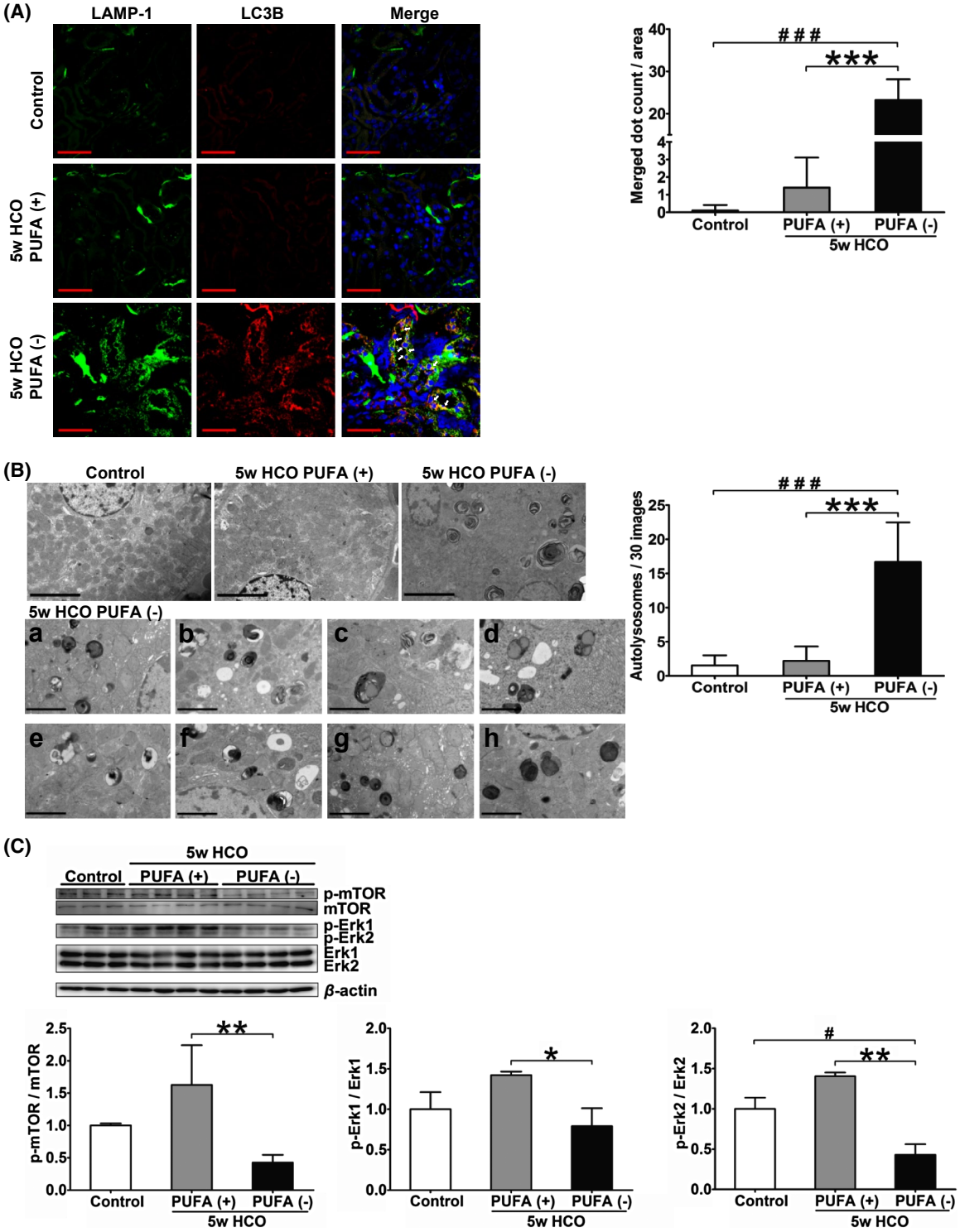

FIGURE 7 A PUFA-deficient diet induces autophagy in the renal cortex of C57BL/6 mice. A, Co-localization of LC3B with LAMP-1 in the kidney. Samples were subjected to immunofluorescence for LAMP-1 (green), LC3B (red), and DAPI (blue). Arrows indicate co-localization of LC3B and LAMP-1. Scale bar represents 50 μm. The number of LC3B + LAMP-1 merged dots was counted in at least 10 high-power fields of kidneys in each group. B, The number of autolysosomes was counted in at least 30 images in 5w HCO PUFA (+) and 5w HCO PUFA (−) mice and compared. Scale bar represents 5 μm. a-h: Classical autophagic structures are seen in 5w HCO PUFA (−) mice. Scale bar represents 2.5 μm. (C) Relative ratios of total protein and phosphorylation levels of mTOR and Erk1/2 were examined by immunoblot and densitometric analyses. All data are provided as the mean ± SD (n = 3-4). Statistically significant differences by ANOVA with Tukey's *post hoc* test: $^{*}P < .05$, $^{**}P < .01$, $^{***}P < .001$ vs PUFA (+) group; $^{\#}P < .05$, $^{\#\#\#}P < .001$ vs control group

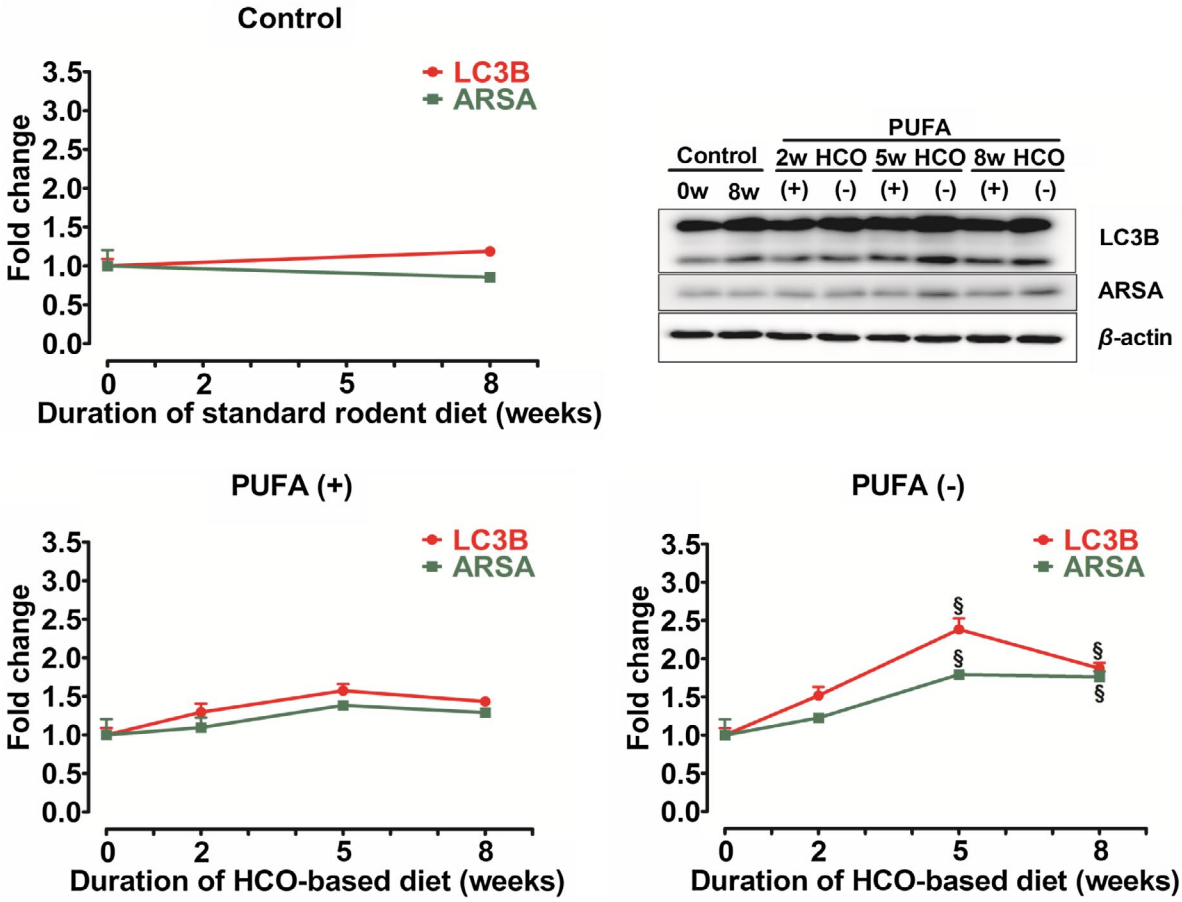

FIGURE 8 Time-course changes in the expression levels of ARSA and LC3B in the kidney. The protein expression levels of ARSA and LC3B were examined by immunoblot and gray analyses. Protein levels were normalized to that of β-actin. All data are shown as fold changes relative to the control group at 0 weeks. Data are expressed as the mean ± SD (n = 3-4). *P* values comparing each time point with control mice of 0 weeks were calculated by the unpaired Student's *t* test: $^{\S}P < .05$

of lysosomal enzyme gene expression via this process. Recently, a combination of genomic analyses identified 471 TFEB direct targets that represented essential components of the CLEAR network. Interestingly, those analyses found that GALC may not belong to the CLEAR network.[51] In the current study, a PUFA deficiency increased the protein expression of GALC without gene upregulation, suggesting that protein expression enhancement of GALC may be strongly affected by systems other than the CLEAR network. An increase in protein expression without gene upregulation was also seen for ARSA. Currently, no reports have addressed the relationship between ARSA and the CLEAR network, ARSA also may not belong to the network. The mechanism of the increased protein expression of GALC and ARSA without gene upregulation is currently unclear. We speculate that increases in these proteins may be influenced by the attenuation of proteolysis. Past studies have shown an inverse relationship between the ubiquitin-proteasome system (UPS) and autophagy, which functionally cooperate with each other to maintain protein stability.[52] The UPS is a selective proteolytic system in which substrates are recognized and labeled by ubiquitin for proteasome degradation. Many reports have demonstrated that autophagy activation attenuates UPS, and that UPS inhibition promotes autophagy conversely.[53,54] Another study identified ARSA as a ubiquitination substrate.[55] Together, those findings suggest the possibility that a PUFA deficiency may attenuate UPS and suppress the proteolysis of ARSA and GALC associated with autophagy activation, followed next by protein expression increases of these enzymes without gene upregulation. Further investigation of this hypothesis is needed.

It was earlier found that the brain content of sulfatides became decreased without synthetic deficiency in the early clinical stage of AD patients, whereas that of ceramides, which are degradation products of sulfatides, was elevated, suggesting the augmentation of sulfatide degradation in the AD brain.[9] Other past studies reported alterations in the intracerebral content of sulfated GAGs in AD. In the cerebral cortex of AD model mice, the total amount of CS was reduced to 56% of the level in control mice.[56] Another report demonstrated that KS levels in the cerebral cortex were decreased to less than half of control levels in AD patients.[57]

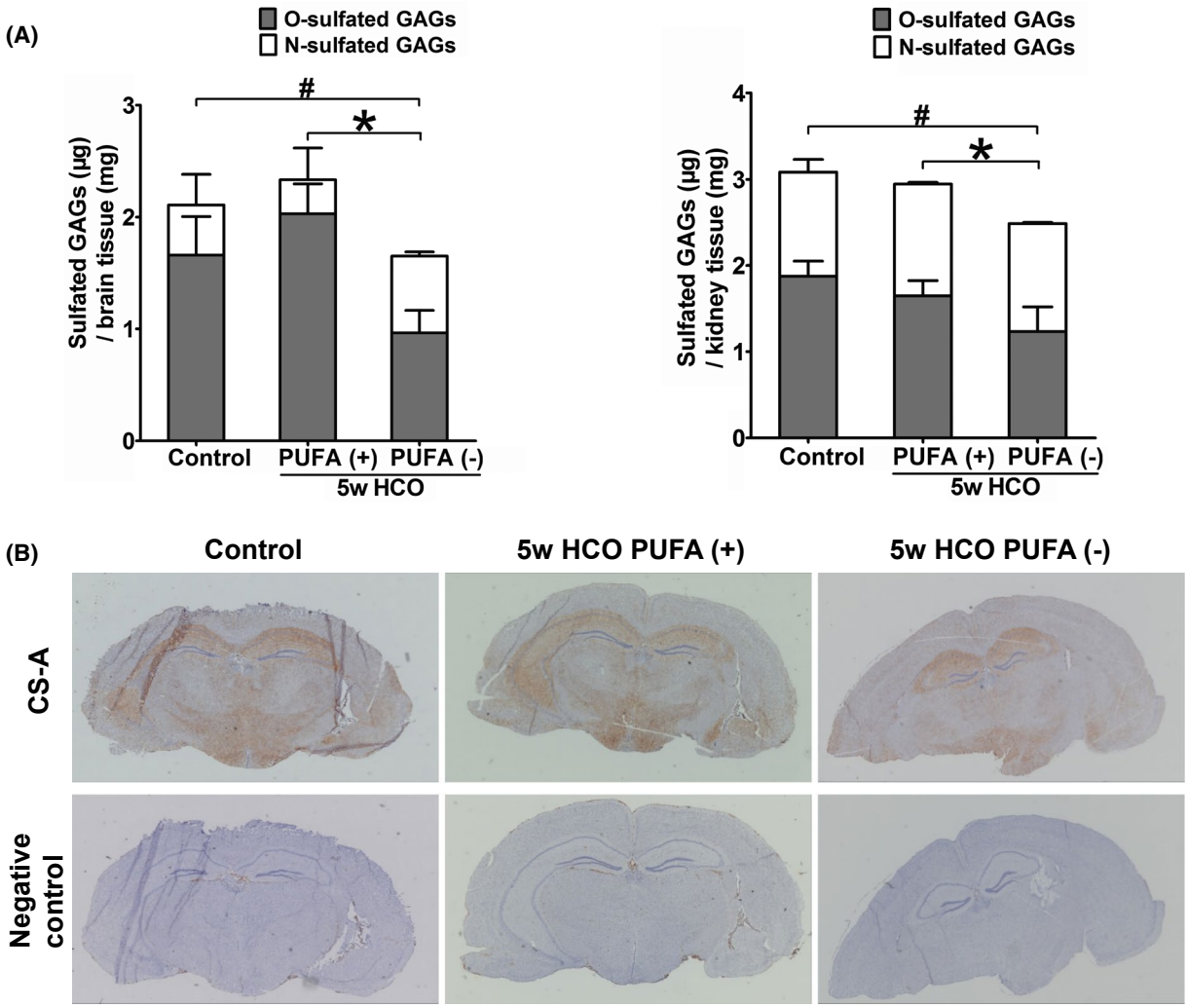

FIGURE 9 A PUFA-deficient diet reduces representative lysosomal enzyme substrates, GAGs, in the brain and kidney. A, Levels of GAGs classified as O-sulfated and N-sulfated glycans in the brain and kidney were measured by the Blyscan Sulfated Glycosaminoglycan Assay. Data are expressed as the mean ± SD (n = 3-4). Statistically significant differences by ANOVA with Tukey's *post hoc* test: $^{*}P < .05$ vs PUFA (+) group; $^{\#}P < .05$ vs control group. B, Immunohistochemical analysis of CS-A in the brain of 5-week-old male C57BL/6 mice. Note that nonspecific weak background staining was found in the colloid plexus and capillaries in the negative control experiment

Moreover, HS, a type of N-sulfated GAG, was accumulated in early Aβ deposition lesions in AD patients.[58,59] The present study demonstrated that a PUFA-deficient diet caused a reduction in brain sulfatide levels, the stimulation of sulfatide degradation, decreases in O-sulfated GAG levels, and a slight increase in N-sulfated GAGs in the brain. Our investigation also uncovered that a PUFA deficiency led to the activation of autophagy and lysosome enzymes in the thalamus- and hypothalamus-containing brain stem, which are the main regions where memory loss and metabolic abnormalities occur in the early stages of AD.[60-62] These current results might be helpful in elucidating the pathological processes of early AD. Past studies have shown that autophagy plays a dual role in Aβ metabolism, participating in both the degradation and generation of Aβ. Autophagy was reported to have a degradative role on Aβ, whereas several studies demonstrated that autophagic vacuoles contained the proteases and substrates necessary to cleave the APP to the Aβ peptide, thus stimulating Aβ generation. The degradation of APP is responsible for regulating synaptic plasticity and memory,[63,64] and autophagosomes are thought to be potentially highly active compartments of Aβ generation.[65] The involvement of autophagy in the balance of Aβ generation and degradation may be influenced by an activation mechanism and/or inducer of autophagy. Our study could not detect a direct effect of a PUFA deficiency on Aβ accumulation. However, we found APP degradation associated with autophagy activation in the PUFA-deficient group, suggesting the stimulation of Aβ generation. In addition, our study detected sulfatide degradation in the PUFA-deficient group. Earlier studies demonstrated that sulfatides promoted the clearance of Aβ through an endocytotic pathway mediated by apolipoprotein E, and its metabolite, ceramide, could stabilize β-site amyloid precursor protein-cleaving enzyme 1 to promote the formation

of Aβ.[66,67] Thus, the sulfatide degradation induced by a PUFA deficiency might reduce the clearance ability of Aβ. Furthermore, past studies reported that CS, a representative O-sulfated GAG and major component of the extracellular matrix, exerted neuroprotective effect and could attenuate the neurotoxicity induced by Aβ25-35, thereby inhibiting fibrinogenesis and shortening the pre-formed amyloid fibrils in the Aβ accumulation pathway of AD.[68,69] CS has also been shown to impart anti-oxidative effects and play an important role in neuroprotection.[70] Oxidative stress may be a risk factor for many neurodegenerative diseases, such as AD. We speculate that a PUFA deficiency causes autophagy activation and the degradation of sulfatides and sulfated GAGs, which exert a positive effect on Aβ generation and accumulation as well as a negative impact on neuroprotection, resulting in a possible AD risk.

In addition to AD, autophagy has been associated with other brain diseases, such as cerebral infarction and PD. Several studies reported that autophagy enhanced secondary neuronal damage in the ipsilateral thalamus after focal cerebral infarction.[71-73] In pathological analyses, autophagosome accumulation was detected in postmortem brain samples of PD, suggesting a pathogenic role of autophagy activation in PD.[74,75] Also in PD, sulfatide levels were considerably decreased in the frontal cortex,[10] and GAGs were reported to exert various effects against α-synuclein aggregation in PD pathogenesis.[76] Moreover, abnormal CS structure and content are commonly observed in the pathological states of schizophrenia.[77] Hence, PUFA-induced autophagy activation and metabolic dysregulations in sulfatides and sulfated glycans may be a potential risk factor for many brain diseases, including AD, cerebral infarction, PD, and schizophrenia.

The current study demonstrated that a PUFA deficiency-induced decrease in sulfatides and sulfated glycans associated with the stimulation of autophagy and lysosomal enzyme activation also occurred in another sulfatide-rich organ, the kidney. Since sulfatides play a role in acid-base homeostasis, diminished renal sulfatides may also be important in metabolic acidosis and chronic kidney disease. A reduction in renal sulfatide content and the stimulation of autophagy have been observed in polycystic kidney diseases.[13,78] Considering the results of our experiments, the decrease in sulfatides in polycystic kidney diseases may have been caused by autophagy stimulation. In the kidney, many studies have described the renoprotective effects of GAGs. GAG treatment prevents the development of kidney disease in subtotal nephrectomy models of chronic kidney disease. Moreover, diabetic rodent models demonstrated that a diabetic condition significantly decreased CS/DS levels in the kidney cortex, and that those sulfated GAGs contributed to reducing albuminuria and glomerulosclerosis.[79] The renoprotective mechanism of GAGs is indeed the subject of many studies.[80] In the kidney disease process, autophagy is reported to play dual pathogenic roles,[81] whereby continuous autophagy activation may lead to renal tubular atrophy and the promotion of renal fibrosis. Autophagy was reported to prevent fibrosis as well by regulating excessive intracellular collagen degradation.[82] The current study could not definitively detect PUFA deficiency-induced kidney functional abnormalities or pathological changes indicative of kidney disease; however, the autophagy activation and decreased levels of sulfatides and sulfated glycans presumably disturbed kidney function in the test animals, possibly leading to future illness. The pathogenic importance of PUFA deficiency-induced autophagy and the degradation of sulfatides and sulfated glycans remains unclear in kidney diseases and requires further study. As a PUFA deficiency can influence general lysosomal function in multiple organs, further systemic studies are needed.

Extensive evidence supports mTOR as a core regulator of autophagy. mTOR can integrate various signals in response to diverse environmental conditions involving four main inputs: nutrients, energy, growth factors, and stress.[83] The molecular mechanism in the mTOR response via the Akt and/or MAPK/Erk1/2 signaling pathways that are mainly regulated by growth factors has been well described. Moreover, mTOR is suppressed by an AMPK-dependent pathway when cells respond to environmental stress or upon energy deprivation.[84] Several upstream signaling cues converge on TSC1-TSC2, which acts as a heterodimer that negatively regulates mTOR signaling. However, the mechanism of how nutrient status is sensed and communicated to mTOR is elusive. For example, oleate-induced noncanonical autophagy was reported to proceed along with the inhibition of mTOR without influence from the downregulation of AMPK, which triggered mechanistically distinct autophagic responses compared with palmitate-induced autophagy.[85] Studies speculate that this noncanonical autophagy characterized by Beclin1-independent autophagic responses has health-promoting effects.[86,87] The present investigation revealed that a PUFA deficiency could induce autophagy through restriction of the Erk/mTOR signaling pathway. This is the first evidence on how mTOR perceives a nutritional deprivation of PUFA to induce autophagy. A better understanding on the mechanism of PUFA deficiency-induced autophagy may contribute to novel therapies for related diseases.

Previous studies have described the preventive effects of PUFA as an essential nutritional supplement for AD. n-3 PUFA can significantly promote interstitial Aβ clearance from the brain and resist Aβ injury by mediating the function of the glymphatic system.[88] In addition, an n-6 PUFA diet can suppress the proteolytic processing of APP to attenuate Aβ deposition.[89] Dietary and lifestyle guidelines have recommended an increase in PUFA intake for the prevention of AD.[24,90] Moreover, a higher dietary intake of DHA has been associated with a lower risk of neurological diseases with inflammatory components in humans, including PD and

severe depression.[91] In the kidney, increasing clinical evidence suggests that n-3 PUFA supplementation has therapeutic potential in reducing proteinuria and kidney dysfunction in IgA nephropathy and other chronic kidney diseases and in reducing inflammation in dialysis patients.[92,93] n-3 PUFA supplementation also appeared to diminish nephrotoxicity and the attendant complication of hypertension toward the inhibition of inflammatory and atherogenic mechanisms in lupus nephritis.[94] The current study suggested that a deficiency in PUFA might cause pathological damage in vivo, with PUFA supplementation exerting protective effects in the same pathological situation. Our findings provide supportive evidence on the possible beneficial effects of PUFA for brain and/or kidney disease prevention.

5 | LIMITATIONS

First, the causal relationship between autophagy activation and the degradation of sulfatides and sulfated GAGs was not fully demonstrated in the present study. Additional experiments investigating the effect of autophagy inhibition on the breakdown of sulfatides and sulfated GAGs in PUFA-deficient mice and cultured cells are necessary. Second, the current study could not clearly demonstrate PUFA deficiency-derived pathogenic effects leading to central nervous system or kidney diseases, such as Aβ deposition or kidney damage. Since the lack of organ damage may be due to a short-term study design, longer trials are needed. Third, this study could not evaluate for synaptic function abnormality. In AD patients, the protection of synaptic function and maintenance of neuronal homeostasis is essential. Sulfatides and other sulfated glycans in the nervous system have many functional properties of membrane proteins, such as ion pumps, myelinated axon ion channels, receptors, and transporters. A severe deficiency in sulfatides and other sulfated glycans is thought to cause losses in axonal conduction and adversely affect synaptic plasticity and memory.[95,96] Since a decrease in the brain content of sulfatides and sulfated GAGs may be a signal of compromised neural network homeostasis, future studies should evaluate these synaptic function abnormalities from a PUFA deficiency.

6 | CONCLUSION

In conclusion, this investigation clearly demonstrated that a PUFA deficiency could lead to the degradation of sulfatides and sulfated GAGs, which may associate with lysosomal hyperfunction and autophagy activation in the brain and kidney, possibly due to inhibition of the Erk/mTOR signaling pathway. General lysosomal hyperfunction with autophagy activation and the associated reduction of a series of functional molecules may result in various diseases, indicating a potential benefit of prophylactic PUFA supplementation.

ACKNOWLEDGMENTS

We thank Dr Nanqi Cui, Dr Ran Guo, and the Research Center for Supports to Advanced Science (Shinshu University School of Medicine) for their invaluable help, advice, instruction, and encouragement. We also thank Ms Tomoko Nishizawa and Ms Yoshiko Sato (Shinshu University School of Medicine) for their invaluable help in the pathological analyses.

CONFLICT OF INTEREST

The authors declare that they have no conflict of interest.

AUTHOR CONTRIBUTIONS

Y. Kamijo, T. Nakajima, and T. Aoyama designed research. Y. Wang and P. Diao performed the experiments and analyzed the data. N. Tanaka, K. Nakamura, and Y. Yamada gave advice on the experiments. J. Nakayama gave advice and performed pathological analyses of GAGs. Y. Wang and Y. Kamijo wrote the manuscript. Y. Kamijo supervised the project. All authors critically reviewed the manuscript.

REFERENCES

1. Marsching C, Eckhardt M, Grone HJ, Sandhoff R, Hopf C. Imaging of complex sulfatides SM3 and SB1a in mouse kidney using MALDI-TOF/TOF mass spectrometry. *Anal Bioanal Chem*. 2011;401:53-64.
2. Xiao S, Finkielstein CV, Capelluto DG. The enigmatic role of sulfatides: new insights into cellular functions and mechanisms of protein recognition. *Adv Exp Med Biol*. 2013;991:27-40.
3. Ishizuka I. Chemistry and functional distribution of sulfoglycolipids. *Prog Lipid Res*. 1997;36:245-319.
4. Honke K, Hirahara Y, Dupree J, et al. Paranodal junction formation and spermatogenesis require sulfoglycolipids. *Proc Natl Acad Sci USA*. 2002;99:4227-4232.
5. Takahashi T, Suzuki T. Role of sulfatide in normal and pathological cells and tissues. *J Lipid Res*. 2012;53:1437-1450.
6. Jeon SB, Yoon HJ, Park SH, Kim IH, Park EJ. Sulfatide, a major lipid component of myelin sheath, activates inflammatory responses as an endogenous stimulator in brain-resident immune cells. *J Immunol*. 2008;181:8077-8087.
7. Jonsson M, Zetterberg H, Rolstad S, et al. Low cerebrospinal fluid sulfatide predicts progression of white matter lesions: the LADIS study. *Dement Geriatr Cogn Disord*. 2012;34:61-67.
8. Cheng H, Wang M, Li JL, Cairns NJ, Han X. Specific changes of sulfatide levels in individuals with pre-clinical Alzheimer's disease: an early event in disease pathogenesis. *J Neurochem*. 2013;127:733-738.
9. Han X, M. Holtzman D, W. McKeel D, Kelley J, Morris JC. Substantial sulfatide deficiency and ceramide elevation in very early Alzheimer's disease: potential role in disease pathogenesis. *J Neurochem*. 2002;82:809-818.
10. Fabelo N, Martin V, Santpere G, et al. Severe alterations in lipid composition of frontal cortex lipid rafts from Parkinson's disease and incidental Parkinson's disease. *Mol Med*. 2011;17:1107-1118.

11. Stettner P, Bourgeois S, Marsching C, et al. Sulfatides are required for renal adaptation to chronic metabolic acidosis. *Proc Natl Acad Sci USA*. 2013;110:9998-10003.
12. Zalc B, Helwig JJ, Ghandour MS, Sarlieve L. Sulfatide in the kidney: how is this lipid involved in sodium chloride transport? *FEBS Lett*. 1978;92:92-96.
13. Deshmukh GD, Radin NS, Gattone VH 2nd, Shayman JA. Abnormalities of glycosphingolipid, sulfatide, and ceramide in the polycystic (cpk/cpk) mouse. *J Lipid Res*. 1994;35:1611-1618.
14. Kim IC, Bang G, Lee JH, et al. Low C24-OH and C22-OH sulfatides in human renal cell carcinoma. *J Mass Spectrom*. 2016;51:182.
15. Kadomatsu K, Sakamoto K. Mechanisms of axon regeneration and its inhibition: roles of sulfated glycans. *Arch Biochem Biophys*. 2014;558:36-41.
16. Maeda N, Ishii M, Nishimura K, Kamimura K. Functions of chondroitin sulfate and heparan sulfate in the developing brain. *Neurochem Res*. 2011;36:1228-1240.
17. Harvey SJ. Models for studies of proteoglycans in kidney pathophysiology. *Methods Mol Biol*. 2012;836:259-284.
18. Lensen JF, Rops AL, Wijnhoven TJ, et al. Localization and functional characterization of glycosaminoglycan domains in the normal human kidney as revealed by phage display-derived single chain antibodies. *J Am Soc Nephrol*. 2005;16:1279-1288.
19. Lemos CC, Tovar AM, Guimaraes MA, Bregman R. Effect of castration on renal glycosaminoglycans and their urinary excretion in male and female rats with chronic renal failure. *Braz J Med Biol Res*. 2013;46:567-573.
20. Innis SM. Essential fatty acids in growth and development. *Prog Lipid Res*. 1991;30:39-103.
21. Spector AA, Kim HY. Discovery of essential fatty acids. *J Lipid Res*. 2015;56:11-21.
22. Lafourcade M, Larrieu T, Mato S, et al. Nutritional omega-3 deficiency abolishes endocannabinoid-mediated neuronal functions. *Nat Neurosci*. 2011;14:345-350.
23. Su HM. Mechanisms of n-3 fatty acid-mediated development and maintenance of learning memory performance. *J Nutr Biochem*. 2010;21:364-373.
24. Thomas J, Thomas CJ, Radcliffe J, Itsiopoulos C. Omega-3 fatty acids in early prevention of inflammatory neurodegenerative disease: a focus on Alzheimer's disease. *Biomed Res Int*. 2015;2015:172801.
25. De Caterina R, Endres S, Kristensen SD, Schmidt EB. n-3 fatty acids and renal diseases. *Am J Kidney Dis*. 1994;24:397-415.
26. Lu J, Bankovic-Calic N, Ogborn M, Saboorian MH, Aukema HM. Detrimental effects of a high fat diet in early renal injury are ameliorated by fish oil in Han:SPRD-cy rats. *J Nutr*. 2003;133:180-186.
27. Sharma A, Hye Khan MA, Levick SP, Lee KS, Hammock BD, Imig JD. Novel omega-3 fatty acid epoxygenase metabolite reduces kidney fibrosis. *Int J Mol Sci*. 2016;17:751.
28. Nakajima T, Yang Y, Lu Y, et al. Decreased fatty acid beta-oxidation is the main cause of fatty liver induced by polyunsaturated fatty acid deficiency in mice. *Tohoku J Exp Med*. 2017;242:229-239.
29. Hara A, Radin NS. Lipid extraction of tissues with a low-toxicity solvent. *Anal Biochem*. 1978;90:420-426.
30. Li G, Hu R, Kamijo Y, et al. Establishment of a quantitative, qualitative, and high-throughput analysis of sulfatides from small amounts of sera by matrix-assisted laser desorption ionization-time of flight mass spectrometry. *Anal Biochem*. 2007;362:1-7.
31. Cheng H, Sun G, Yang K, Gross RW, Han X. Selective desorption/ionization of sulfatides by MALDI-MS facilitated using 9-aminoacridine as matrix. *J Lipid Res*. 2010;51:1599-1609.
32. Yamada Y, Harada M, Hashimoto K, et al. Impact of chronic kidney dysfunction on serum Sulfatides and its metabolic pathway in mice. *Glycoconj J*. 2019;36:1-11.
33. Aoyama T, Peters JM, Iritani N, et al. Altered constitutive expression of fatty acid-metabolizing enzymes in mice lacking the peroxisome proliferator-activated receptor alpha (PPARalpha). *J Biol Chem*. 1998;273:5678-5684.
34. Sukegawa K, Orii T. Quantitation and biosynthesis of beta-glucuronidase cross-reactive material in fibroblasts from patients with mucopolysaccharidosis VII. *J Inherit Metab Dis*. 1985;8:145-146.
35. Kamijo Y, Hora K, Tanaka N, et al. Identification of functions of peroxisome proliferator-activated receptor alpha in proximal tubules. *J Am Soc Nephrol*. 2002;13:1691-1702.
36. Kamijo Y, Hora K, Kono K, et al. PPARalpha protects proximal tubular cells from acute fatty acid toxicity. *J Am Soc Nephrol*. 2007;18:3089-3100.
37. Li X, Kurita H, Xiao T, Iijima K, Kurashina K, Nakayama J. Potential involvement of chondroitin sulfate A in the pathogenesis of ameloblastoma. *Acta Histochem*. 2017;119:439-445.
38. Dunlop EA, Tee AR. mTOR and autophagy: a dynamic relationship governed by nutrients and energy. *Semin Cell Dev Biol*. 2014;36:121-129.
39. Cheng B, Lu J, Li T, et al. 1,3-Dichloro-2-Propanol inhibits autophagy via P53/AMPK/mTOR pathway in HepG2 cells. *Food Chem Toxicol*. 2018;122:143-150.
40. Egan D, Kim J, Shaw RJ, Guan KL. The autophagy initiating kinase ULK1 is regulated via opposing phosphorylation by AMPK and mTOR. *Autophagy*. 2011;7:643-644.
41. Hu B, Zhang Y, Jia L, et al. Binding of the pathogen receptor HSP90AA1 to avibirnavirus VP2 induces autophagy by inactivating the AKT-MTOR pathway. *Autophagy*. 2015;11:503-515.
42. Sun Y, Zou M, Hu C, et al. Wogonoside induces autophagy in MDA-MB-231 cells by regulating MAPK-mTOR pathway. *Food Chem Toxicol*. 2013;51:53-60.
43. Zhang B, Song Y, Sun S, et al. Human papillomavirus 11 early protein E6 activates autophagy by repressing AKT/mTOR and Erk/mTOR. *J Virol*. 2019;93(12):1-16.
44. Nixon RA, Wegiel J, Kumar A, et al. Extensive involvement of autophagy in Alzheimer disease: an immuno-electron microscopy study. *J Neuropathol Exp Neurol*. 2005;64:113-122.
45. Han X. The pathogenic implication of abnormal interaction between apolipoprotein E isoforms, amyloid-beta peptides, and sulfatides in Alzheimer's disease. *Mol Neurobiol*. 2010;41:97-106.
46. Vogler C, Galvin N, Levy B, et al. Transgene produces massive overexpression of human beta -glucuronidase in mice, lysosomal storage of enzyme, and strain-dependent tumors. *Proc Natl Acad Sci USA*. 2003;100:2669-2673.
47. Li H, Peng X, Wang Y, et al. Atg5-mediated autophagy deficiency in proximal tubules promotes cell cycle G2/M arrest and renal fibrosis. *Autophagy*. 2016;12:1472-1486.
48. Ashabi G, Ahmadiani A, Abdi A, Abraki SB, Khodagholi F. Time course study of Abeta formation and neurite outgrowth disruption in differentiated human neuroblastoma cells exposed to H2O2: protective role of autophagy. *Toxicol In Vitro*. 2013;27:1780-1788.
49. Settembre C, Zoncu R, Medina DL, et al. A lysosome-to-nucleus signalling mechanism senses and regulates the lysosome via mTOR and TFEB. *EMBO J*. 2012;31:1095-1108.

50. Settembre C, Di Malta C, Polito VA, et al. TFEB links autophagy to lysosomal biogenesis. *Science*. 2011;332:1429-1433.
51. Palmieri M, Impey S, Kang H, et al. Characterization of the CLEAR network reveals an integrated control of cellular clearance pathways. *Hum Mol Genet*. 2011;20:3852-3866.
52. Schreiber A, Peter M. Substrate recognition in selective autophagy and the ubiquitin-proteasome system. *Biochem Biophys Acta*. 2014;1843:163-181.
53. Kocaturk NM, Gozuacik D. Crosstalk between mammalian autophagy and the ubiquitin-proteasome system. *Front Cell Dev Biol*. 2018;6:128.
54. Sun Y, Grabowski GA. Altered autophagy in the mice with a deficiency of saposin A and saposin B. *Autophagy*. 2013;9:1115-1116.
55. Kelsey KM, Zigo M, Thompson WE, et al. Reciprocal surface expression of arylsulfatase A and ubiquitin in normal and defective mammalian spermatozoa. *Cell Tissue Res*. 2020;379:561-576.
56. Zhang Z, Ohtake-Niimi S, Kadomatsu K, Uchimura K. Reduced molecular size and altered disaccharide composition of cerebral chondroitin sulfate upon Alzheimer's pathogenesis in mice. *Nagoya J Med Sci*. 2016;78:293-301.
57. Lindahl B, Eriksson L, Spillmann D, Caterson B, Lindahl U. Selective loss of cerebral keratan sulfate in Alzheimer's disease. *J Biol Chem*. 1996;271:16991-16994.
58. Snow AD, Mar H, Nochlin D, et al. Early accumulation of heparan sulfate in neurons and in the beta-amyloid protein-containing lesions of Alzheimer's disease and Down's syndrome. *Am J Pathol*. 1990;137:1253-1270.
59. Huynh MB, Ouidja MO, Chantepie S, et al. Glycosaminoglycans from Alzheimer's disease hippocampus have altered capacities to bind and regulate growth factors activities and to bind tau. *PLoS One*. 2019;14:e0209573.
60. Aggleton JP, Pralus A, Nelson AJ, Hornberger M. Thalamic pathology and memory loss in early Alzheimer's disease: moving the focus from the medial temporal lobe to Papez circuit. *Brain*. 2016;139:1877-1890.
61. Ishii M, Iadecola C. Metabolic and non-cognitive manifestations of Alzheimer's disease: the hypothalamus as both culprit and target of pathology. *Cell Metab*. 2015;22:761-776.
62. Zheng H, Zhou Q, Du Y, et al. The hypothalamus as the primary brain region of metabolic abnormalities in APP/PS1 transgenic mouse model of Alzheimer's disease. *Biochim Biophys Acta Mol Basis Dis*. 2018;1864:263-273.
63. Ludewig S, Korte M. Novel insights into the physiological function of the APP (Gene) family and its proteolytic fragments in synaptic plasticity. *Front Mol Neurosci*. 2016;9:161.
64. Rice HC, de Malmazet D, Schreurs A, et al. Secreted amyloid-beta precursor protein functions as a GABABR1a ligand to modulate synaptic transmission. *Science*. 2019;363:1-7.
65. Yu WH, Kumar A, Peterhoff C, et al. Autophagic vacuoles are enriched in amyloid precursor protein-secretase activities: implications for beta-amyloid peptide over-production and localization in Alzheimer's disease. *Int J Biochem Cell Biol*. 2004;36:2531-2540.
66. Puglielli L, Ellis BC, Saunders AJ, Kovacs DM. Ceramide stabilizes beta-site amyloid precursor protein-cleaving enzyme 1 and promotes amyloid beta-peptide biogenesis. *J Biol Chem*. 2003;278:19777-19783.
67. Zeng Y, Han X. Sulfatides facilitate apolipoprotein E-mediated amyloid-beta peptide clearance through an endocytotic pathway. *J Neurochem*. 2008;106:1275-1286.
68. Pollack SJ, Sadler II, Hawtin SR, Tailor VJ, Shearman MS. Sulfonated dyes attenuate the toxic effects of beta-amyloid in a structure-specific fashion. *Neurosci Lett*. 1995;197:211-214.
69. McLaughlin RW, De Stigter JK, Sikkink LA, Baden EM, Ramirez-Alvarado M. The effects of sodium sulfate, glycosaminoglycans, and Congo red on the structure, stability, and amyloid formation of an immunoglobulin light-chain protein. *Protein Sci*. 2006;15:1710-1722.
70. Suttkus A, Morawski M, Arendt T. Protective properties of neural extracellular matrix. *Mol Neurobiol*. 2016;53:73-82.
71. Zhang J, Zhang Y, Li J, et al. Autophagosomes accumulation is associated with beta-amyloid deposits and secondary damage in the thalamus after focal cortical infarction in hypertensive rats. *J Neurochem*. 2012;120:564-573.
72. Xing S, Zhang Y, Li J, et al. Beclin 1 knockdown inhibits autophagic activation and prevents the secondary neurodegenerative damage in the ipsilateral thalamus following focal cerebral infarction. *Autophagy*. 2012;8:63-76.
73. Li Y, Zhang J, Chen L, et al. Ebselen reduces autophagic activation and cell death in the ipsilateral thalamus following focal cerebral infarction. *Neurosci Lett*. 2015;600:206-212.
74. Dehay B, Bove J, Rodriguez-Muela N, et al. Pathogenic lysosomal depletion in Parkinson's disease. *J Neurosc*. 2010;30:12535-12544.
75. Su LY, Li H, Lv L, et al. Melatonin attenuates MPTP-induced neurotoxicity via preventing CDK5-mediated autophagy and SNCA/alpha-synuclein aggregation. *Autophagy*. 2015;11:1745-1759.
76. Mehra S, Ghosh D, Kumar R, et al. Glycosaminoglycans have variable effects on alpha-synuclein aggregation and differentially affect the activities of the resulting amyloid fibrils. *J Biol Chem*. 2018;293:12975-12991.
77. Miyata S, Kitagawa H. Chondroitin sulfate and neuronal disorders. *Front Biosci*. 2016;21:1330-1340.
78. Belibi F, Zafar I, Ravichandran K, et al. Hypoxia-inducible factor-1alpha (HIF-1alpha) and autophagy in polycystic kidney disease (PKD). *Am J Physiol Renal Physiol*. 2011;300:F1235-F1243.
79. Reine TM, Grondahl F, Jenssen TG, Hadler-Olsen E, Prydz K, Kolset SO. Reduced sulfation of chondroitin sulfate but not heparan sulfate in kidneys of diabetic db/db mice. *J Histochem Cytochem*. 2013;61:606-616.
80. Masola V, Zaza G, Gambaro G. Sulodexide and glycosaminoglycans in the progression of renal disease. *Nephrol Dial Transpl*. 2014;29(suppl. 1):i74-i79.
81. Melk A, Baisantry A, Schmitt R. The yin and yang of autophagy in acute kidney injury. *Autophagy*. 2016;12:596-597.
82. He L, Livingston MJ, Dong Z. Autophagy in acute kidney injury and repair. *Nephron Clin Pract*. 2014;127:56-60.
83. Kim SG, Buel GR, Blenis J. Nutrient regulation of the mTOR complex 1 signaling pathway. *Mol Cells*. 2013;35:463-473.
84. Wullschleger S, Loewith R, Hall MN. TOR signaling in growth and metabolism. *Cell*. 2006;124:471-484.
85. Niso-Santano M, Malik SA, Pietrocola F, et al. Unsaturated fatty acids induce non-canonical autophagy. *EMBO J*. 2015;34:1025-1041.
86. Bankaitis VA. Unsaturated fatty acid-induced non-canonical autophagy: unusual? Or unappreciated? *EMBO J*. 2015;34:978-980.
87. Niso-Santano M, Bravo-San Pedro JM, Maiuri MC, et al. Novel inducers of BECN1-independent autophagy: cis-unsaturated fatty acids. *Autophagy*. 2015;11:575-577.
88. Ren H, Luo C, Feng Y, et al. Omega-3 polyunsaturated fatty acids promote amyloid-beta clearance from the brain through mediating the function of the glymphatic system. *FASEB J*. 2017;31:282-293.

89. Hosono T, Nishitsuji K, Nakamura T, et al. Arachidonic acid diet attenuates brain Abeta deposition in Tg2576 mice. *Brain Res*. 2015;1613:92-99.
90. Spence J, Chintapenta M, Kwon HI, Blaszczyk AT. A brief review of three common supplements used in Alzheimer's disease. *Consult Pharm*. 2017;32:412-414.
91. Bazinet RP, Laye S. Polyunsaturated fatty acids and their metabolites in brain function and disease. *Nat Rev Neurosci*. 2014;15:771-785.
92. Huang X, Lindholm B, Stenvinkel P, Carrero JJ. Dietary fat modification in patients with chronic kidney disease: n-3 fatty acids and beyond. *J Nephrol*. 2013;26:960-974.
93. Moriyama T, Kumon S, Kamiyama T, Karasawa K, Uchida K, Nitta K. The renoprotective effects of docosahexaenoic acid as an add-on therapy in patients receiving eicosapentaenoic acid as treatment for IgA nephropathy: a pilot uncontrolled trial. *Intern Med*. 2018;57:173-179.
94. Donadio JV Jr. Omega-3 polyunsaturated fatty acids: a potential new treatment of immune renal disease. *Mayo Clin Proc*. 1991;66:1018-1028.
95. Ishibashi T, Dupree JL, Ikenaka K, et al. A myelin galactolipid, sulfatide, is essential for maintenance of ion channels on myelinated axon but not essential for initial cluster formation. *J Neurosci*. 2002;22:6507-6514.
96. Marcus J, Honigbaum S, Shroff S, Honke K, Rosenbluth J, Dupree JL. Sulfatide is essential for the maintenance of CNS myelin and axon structure. *Glia*. 2006;53:372-381.

SUPPORTING INFORMATION

Additional Supporting Information may be found online in the Supporting Information section.

How to cite this article: Wang Y, Nakajima T, Diao P, et al. Polyunsaturated fatty acid deficiency affects sulfatides and other sulfated glycans in lysosomes through autophagy-mediated degradation. *The FASEB Journal*. 2020;00:1–21. https://doi.org/10.1096/fj.202000030RR